NTIA Report 21-556

Solid-state Marine Radar Interference in Magnetron Marine Radars

R. J. Achatz
N. Kent
E. Hill

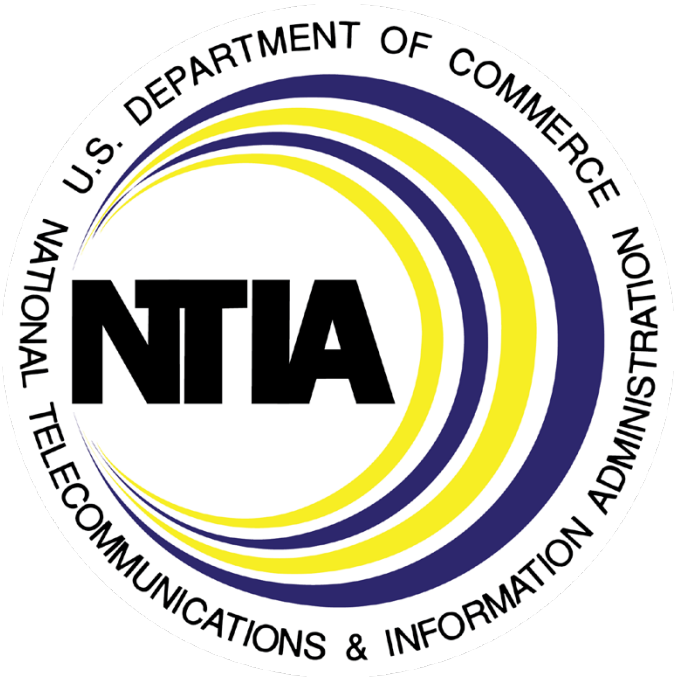

Technical Report

NTIA Report 21-556

Solid-state Marine Radar Interference in Magnetron Marine Radars

R.J. Achatz
N. Kent
E. Hill

U.S. DEPARTMENT OF COMMERCE

Evelyn Remaley
Acting Assistant Secretary of Commerce for Communications and Information
National Telecommunications and Information Administration

July 2021

DISCLAIMER

Certain commercial equipment and materials are identified in this report to specify adequately the technical aspects of the reported results. In no case does such identification imply recommendation or endorsement by the National Telecommunications and Information Administration, nor does it imply that the material or equipment identified is the best available for this purpose.

CONTENTS

FIGURES

TABLES

ABBREVIATIONS/ACRONYMS

μs	microsecond
CFAR	constant false alarm rate
dB	decibel
dBi	decibels relative to isotropic antenna
dBW	decibel relative to Watt
FM	frequency modulation
FMCW	frequency modulated continuous wave
FTC	fast time constant
IMO	International Maritime Organization
INR	interference to noise power ratio
IPC	interference protection criteria
IR	interference rejection
ITS	Institute for Telecommunication Sciences
ITU	International Telecommunication Union
K	Kelvin
kHz	kilohertz
km	kilometer
LCM	lowest common multiple
MHz	megahertz
ML	main lobe
M/N	M out of N
MR	marine radar
M-MR	magnetron marine radar
ms	millisecond
MSD	minimum separation distance
NLFM	nonlinear frequency modulation
NM	nautical mile
ns	nanosecond
NTIA	National Telecommunications and Information Administration
Pd	probability of detection
Pfa	probability of false alarm
PPI	plan position indicator
PRF	pulse repetition frequency
PRI	pulse repetition interval
PSD	power spectral density
PW	pulsed width

RPM	revolutions per minute
RR	rotation rate
SBL	side and back lobes
SNR	signal to noise power ratio
s	seconds
SS	solid state
SS-MR	solid state marine radar
STC	sensitivity time constant
W	watt

EXECUTIVE SUMMARY

Marine radars (MR) used for navigation and surveillance purposes transmit signals whose received reflections determine the locations of various marine objects such as buoys, vessels, icebergs, and shorelines. In the past, MRs used short, low duty-cycle, high power continuous-wave (CW) pulses generated by a magnetron oscillator. Unfortunately the magnetron MR (M-MR) oscillator has a relatively low mean time between failure that increases maintenance costs, high frequency-instability that makes coherent signal processing clutter rejection difficult, and high spurious emissions. Modern solid state MRs (SS-MR) overcome these problems by amplifying longer, high duty-cycle, pulsed frequency-modulated (FM) or FM continuous-wave (FMCW) signals at much lower power levels.

While the SS-MRs offer great potential to marine navigation, it has yet to be established how well they will share spectrum with existing M-MR. Previous tests conducted by ITS have shown that M-MR interference rejection (IR) techniques can mitigate pulsed CW interference with duty cycles as high as 5% but fail to mitigate pulsed CW interference at the higher duty cycles characteristic of pulsed FM SS-MR. Field tests have anecdotally demonstrated that an SS-MR signal can cause interference in M-MR. Analytic research shows that interference is more likely to occur when multiple SS-MRs are present, as they would be in a crowded port or harbor. Clearly there is a need for more interference evaluation now and in the future.

Since improvements to IR techniques are possible but unrealistic given the large number of existing M-MR and crowded port and harbor conditions do not allow distance separation, the best way to mitigate this interference is to develop an interference evaluation method and use it to determine the minimum frequency separation between new SS-MR and legacy M-MR. The purpose of this work is to develop this method and use it to evaluate the previously published field test results.

While field tests are arguably the most realistic interference evaluation approach, they are also the most costly and difficult to replicate by others. Our approach is to model the M-MR and SS-MR signals, implement the models into a radio system software simulation tool, and use the tool to estimate the maximum interference power the victim receiver can tolerate (i.e. its interference protection criteria (IPC)). The IPC is then used in conjunction with the interference link power budget to analytically determine the minimum separation distance (MSD) needed at various frequency separations.

The M-MR receiver model featured double threshold detection, PRI discrimination IR, and short, medium, and long range operational modes. IPC for three SS-MR signals were obtained for each of these modes. MSD were computed at the 50, 5, and 0.5 percentiles of time exceeded based on mutual antenna gain statistics.

The simulations and analysis with IR off and a 55 MHz frequency separation showed that the short range had both the lowest IPC and longest MSDs and therefore was the range most susceptible to SS-MR interference. Short range was also the only range that had significant MSD at the 50 percentile. However, it is worth noting that medium and long range MSD still could be significant at the 5 and 0.5 percentiles.

Simulations and analysis also showed that pulsed FM signals had longer MSD and therefore more interference potential than the FMCW signals at all ranges. Finally, enabling IR and increasing frequency separation from 55 to 135 MHz were both very effective at mitigating the SS-MR interference.

Only short range simulations achieved the high false alarms seen in the field test. Since the field test PPI displays suggested operation in medium range we assumed the field test M-MR radar medium range used a short range bandwidth and its PPI results could be compared to our short range results. Given this and all the other assumed M_MR equipment parameters and SS-MR interfering signal characterisitcs, the simulation and analysis method results seem to support field test results i.e. that IR, frequency separation, and distance separation are fairly effective SS-MR interference mitigation measures.

MRs are not guaranteed interference-free radio spectrum. This is why all M-MR have some sort of IR. Even the simplest PRI discrimination IR used by this method is remarkably effective at removing interference from other M-MRs and these results demonstrated that it is also effective at mitigating interference from a single SS-MR. This finding is important in the event that adequate frequency or distance separations are not available. However, there is a concern that legacy M-MR IR may not be as effective at removing the interference from multiple SS-MRs present in a crowded harbor or port where distance separation is difficult to achieve.

The next logical step for improving this method would be to establish standardized M-MR receiver settings and baseline operating conditions. Analysis also needs to be expanded to include other SS-MR and aggregate SS-MR interfering waveforms.

The numbers and characteristics of new SS-MR signals will inevitably increase with the advances in solid state device and digital signal processing technologies. Some of these new SS-MR signals may have even higher duty cycles than the ones used here. Clearly a method for evaluating the compatibility of these new SS-MR signals is needed. The simulation and analysis method described in this report, which quantifies the maximum interfering signal power and MSD, is a significant first step in this direction.

SOLID-STATE MARINE RADAR INTERFERENCE IN MAGNETRON MARINE RADARS

R.J. Achatz[1], N. Kent,[2] and E. Hill[1]

Previously published field test results showed frequent solid state marine radar (SS-MR) interference in magnetron marine radars (M-MRs) at 0.34 nautical miles distance separation and 55 MHz frequency separation. The interference was mitigated but not completely eliminated by increasing distance separation, activating interference rejection (IR), and increasing frequency separation. This report describes a simulation and analysis method that can emulate the field test and uses the method to evaluate the previously published field test results. Results from the method support those of the field test to a large extent although the method results showed more complete mitigation with frequency separation and IR. The field test was performed with a single SS-MR interferer. Legacy M-MR IR may not be as effective in crowded ports or harbors where there are a number of new SS-MR operating nearby. In addition, new SS-MR signals may have higher duty cycles than the ones used here. This method will be an invaluable tool for determining the necessary frequency separation between legacy M-MR and new SS-MR.

Keywords: interference, interference protection criteria, magnetron marine radar, marine radar, radio navigation radar, radio surveillance radar, solid state marine radar

1. INTRODUCTION

Marine radars (MR) used for navigation and surveillance purposes transmit signals whose received reflections determine the locations of various marine objects such as buoys, vessels, icebergs, and shorelines. In the past, MRs used short, low duty-cycle[3], high power continuous-wave (CW) pulses generated by a magnetron oscillator. Unfortunately the magnetron MR (M-MR) oscillator has a relatively low mean time between failure that increases maintenance costs, high frequency-instability that makes coherent signal processing clutter rejection difficult, and high spurious emissions. Modern solid state MRs (SS-MR) overcome these problems by amplifying longer, high duty-cycle, pulsed frequency-modulated (FM) or FM continuous-wave (FMCW) signals at much lower power levels.

While the SS-MRs offer great potential to marine navigation, it has yet to be established how well they will share spectrum with existing M-MR. Previous tests conducted by ITS summarized in Appendix A have shown that M-MR interference rejection (IR) techniques can mitigate pulsed CW interference with duty cycles as high as 5% but fail to mitigate pulsed CW interference at the higher duty cycles characteristic of pulsed FM SS-MR [1]. Field tests have anecdotally demonstrated that an SS-MR signal can cause interference in M-MR [2]. Analytic research shows that interference is more likely to occur when multiple SS-MRs are present, as they would

[1] The authors are with the Institute for Telecommunication Sciences, National Telecommunications and Information Administration, U.S. Department of Commerce, Boulder, CO 80305.
[2] The author was formerly with the Institute for Telecommunication Sciences, National Telecommunications and Information Administration, U.S. Department of Commerce, Boulder, CO 80305.
[3] Ratio of pulse width to pulse repetition interval

be in a crowded port or harbor [3]. Clearly there is a need for more interference evaluation now and in the future.

Since improvements to IR techniques [4],[5] are possible but unrealistic given the large number of existing M-MR and crowded port and harbor conditions do not allow distance separation, the best way to mitigate this interference is to develop an interference evaluation method and use it to determine the minimum frequency separation between new SS-MR and legacy M-MR. The purpose of this work is to develop this method and use it to evaluate the previously published field test results.

While field tests are arguably the most realistic interference evaluation approach, they are also the most costly and difficult to replicate by others. Our approach is to model the M-MR and SS-MR signals, implement the models into a radio system software simulation tool, and use the tool to estimate the maximum interference power the victim receiver can tolerate (i.e. its interference protection criteria (IPC)). The IPC is then used in conjunction with the interference link power budget to analytically determine the minimum separation distance (MSD) needed at various frequency separations.

The principal risk to this simulation and analysis approach is the computational burden imposed by having to simulate a statistically significant number of interference events despite the fact that asynchronous M-MR and SS-MR pulse trains create a significant amount of "dead time" where neither magnetron or solid state pulses are present. We minimized this computational burden by limiting the number of Monte Carlo trials to the minimum number needed to achieve an acceptable uncertainty. Another risk is the computational burden imposed by having to simulate excessively large frequency ranges because of the wide signal bandwidths and large frequency separations. We minimized this computational burden by using only that portion of the SS-MR signal spectrum that lies in the IPC simulation bandwidth.

This report describes the simulation and analysis method and explains how the method was used to determine IPC and MSD and emulate the previously published field test. Section 2 describes the field test interference scenario, Section 3 describes the M-MR and SS-MR signal models, Section 4 describes the simulation and analysis method, Section 5 shows IPC, MSD, and field test emulation results, and Section 6 summarizes findings.

2. INTERFERENCE SCENARIO

The interference scenario is taken from a field test, conducted at Kiel Harbor in Kiel, Germany on October 21, 2014 [2]. In the field test, a vessel equipped with a M-MR was anchored in a harbor. Another vessel equipped with a SS-MR was driven away from the anchored vessel so that SS-MR interference in the M-MR could be observed at different separation distances. The field test was conducted in the marine radar 9200-9500 MHz band (i.e. the marine radar X-band) in low clutter conditions composed of calm seas and geographically scattered rain showers.

The M-MR was operated at 9375 MHz. As shown in Figure 1, the SS-MR could be tuned to any frequency from 9220 to 9480 MHz in 20 MHz steps. With this scheme, the 9320 MHz "channel", 55 MHz from the 9375 MHz M-MR "channel", is the closest non-overlapping SS-MR channel to the M-MR channel assuming the SS-MR and M-MR channels are 20 and 60 MHz respectively.

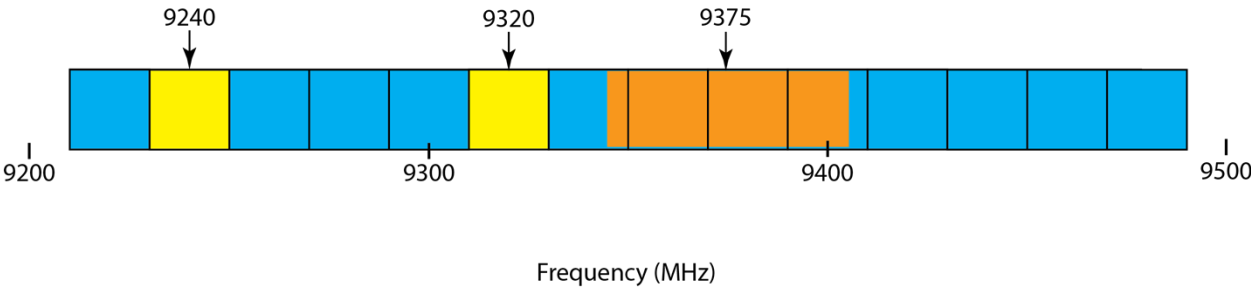

Figure 1. Spectrum scenario. SS-MR channels (yellow) are 20 MHz wide and centered at 9240 or 9320 MHz. M-MR channel (orange) is 60 MHz wide and centered at 9375 MHz.

Field test results were presented with 4 M-MR planned position indicator (PPI) displays that are referred to as PPI 1-4 and reproduced in Figures 2–5. The PPI are dominated by diffuse targets caused by rain showers and dashed radial and spiral ("running rabbits" [8]) interference presumably caused by the SS-MR signal.

The appearance of the interference is dependent on the interfering signal characteristics, its frequency offset from the victim receiver, antenna rotation rates, and antenna gains. The length of the dashes correspond to the interfering pulse width. However, frequency offsetting can shorten the length of the dash sometimes converting on-channel dashes to frequency-offset dots ("rabbit ears" [9]).

For our analysis, PPI 2 has been identified as the "reference" PPI without interference mitigation. The remaining PPIs are identified by the type of interference mitigation applied i.e. frequency separation, IR, or distance separation. This organization is summarized in Table 1. Distances are reported in nautical miles (NM).

Table 1. Field test trial conditions. Shaded boxes highlight difference from reference.

Test	PPI #	Display Range (NM)	SS-MR Frequency (MHz)	Frequency Separation (MHz)	IR status	Distance Separation (NM)
Reference	2	12	9320	55	Off	0.34
Frequency separation	1	6	9240	135	Off	0.34
Interference rejection	3	12	9320	55	On	0.34
Distance separation	4	12	9320	55	Off	2.00

For PPI-2, the reference, radar interference is evident as radials with long dashes at most azimuths and concentric, dotted, circles centered around 90 degrees. Diffuse rain shower targets are centered at 240 degrees.

For PPI-1, the frequency separation test, radar interference is evident as radials with long dashes centered around 135 and 240 degrees. Diffuse rain shower targets are centered at 240 degrees. PPI-1 display range is 6 NM instead of the 12 NM the other PPI have.

For PPI-3, the IR test, radar interference is evident as radials with long dashes centered around 60, 170, and 270 degrees. Diffuse rain shower targets are centered at 240 degrees.

For PPI-4, the distance separation test, radar interference is evident as radials with long dashes centered on 30 and 220 degrees and sparsely dotted spirals centered around 90 and 315 degrees.

The widespread interference in the reference PPI has been reduced to two or three azimuths in the other PPIs. This demonstrates that frequency separation, IR, and distance separation all mitigate SS-MR interference, although none can completely overcome it.

The demonstration is significant but anecdotal because signal, noise, and interfering signal powers and detailed descriptions of SS-MR signals, M-MR receiver settings, and test procedures were not provided. Status of the M-MR receiver clutter mitigation functions (such as fast time constant (FTC), sensitivity time control (STC), scan-to-scan correlation, and tracking discussed in Appendix B) are of particular interest. Also, while the radar interference is presumed to come from SS-MR no ambient radio spectrum measurements were provided to demonstrate that it was the only other radar operating in the vicinity.

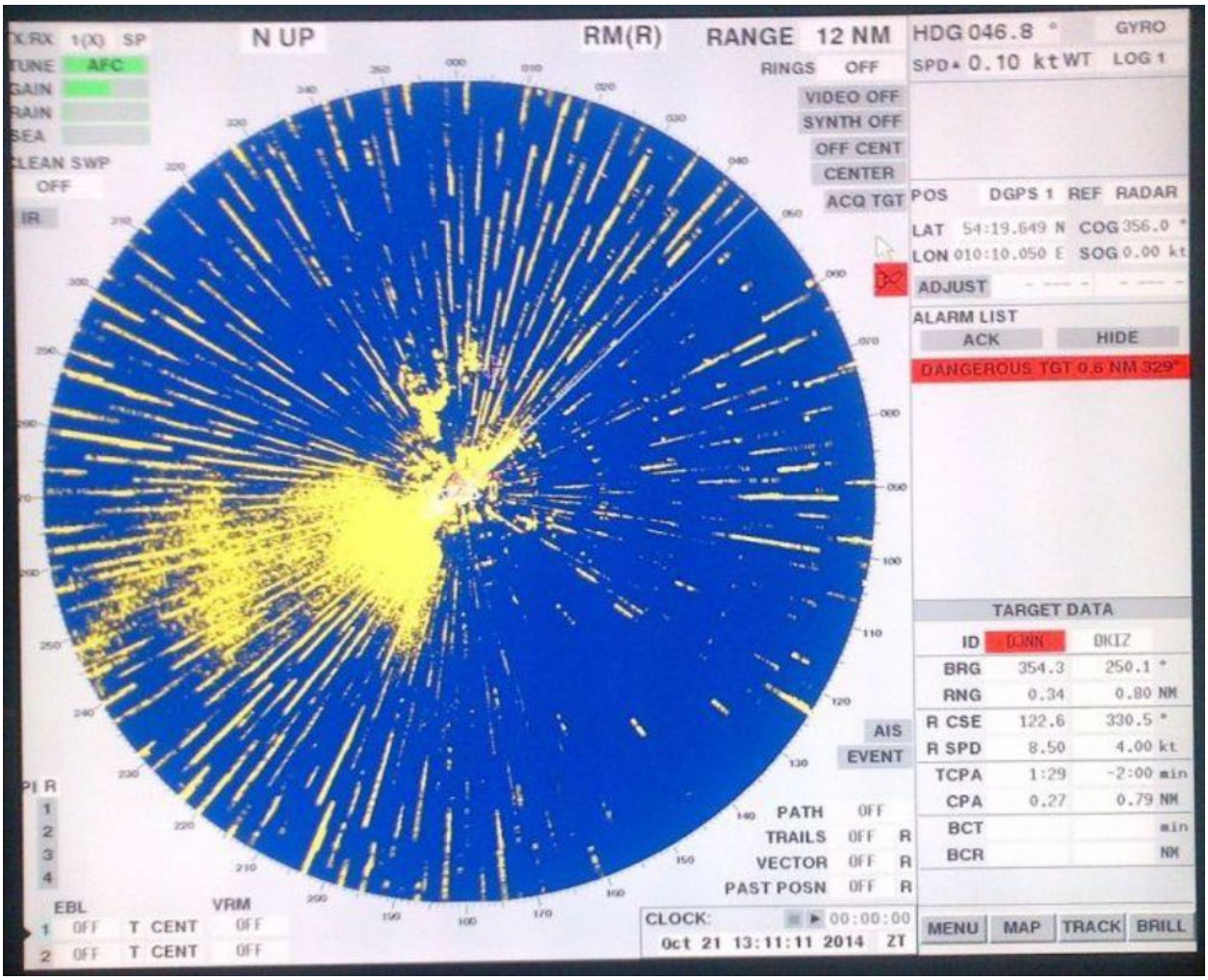

Figure 2. PPI-2, reference. Radar interference is evident as radials with long dashes at most azimuths and concentric, dotted, circles centered around 90 degrees. Diffuse rain shower targets are centered at 240 degrees.

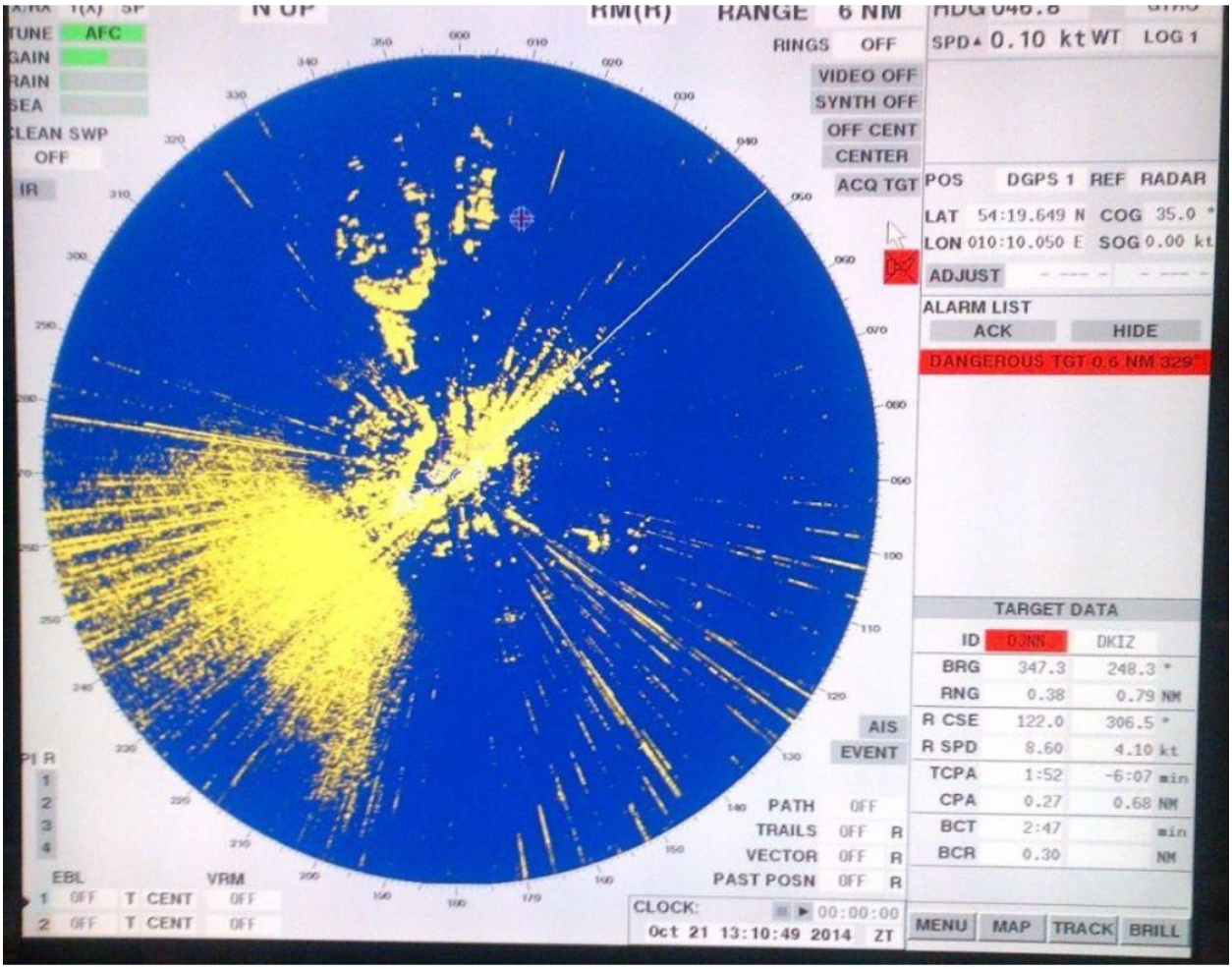

Figure 3. PPI-1, frequency separation test. Radar interference is evident as radials with long dashes centered around 135 and 240 degrees. Diffuse rain shower targets are centered at 240 degrees. PPI-1 display range is 6 NM instead of the 12 NM the other PPI have.

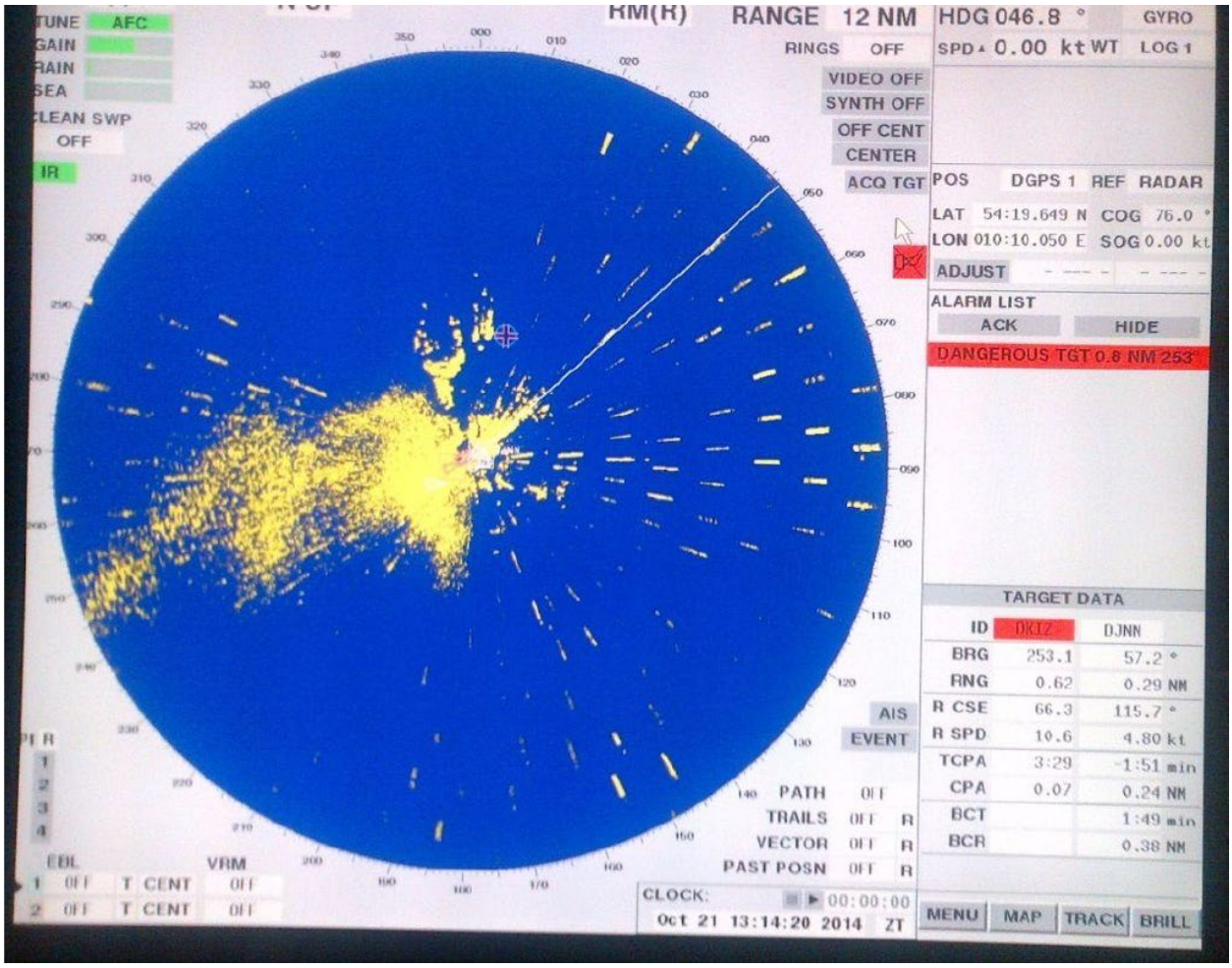

Figure 4. PPI-3, interference reduction test. Radar interference is evident as radials with long dashes centered around 60, 170, and 270 degrees. Diffuse rain shower targets are centered at 240 degrees.

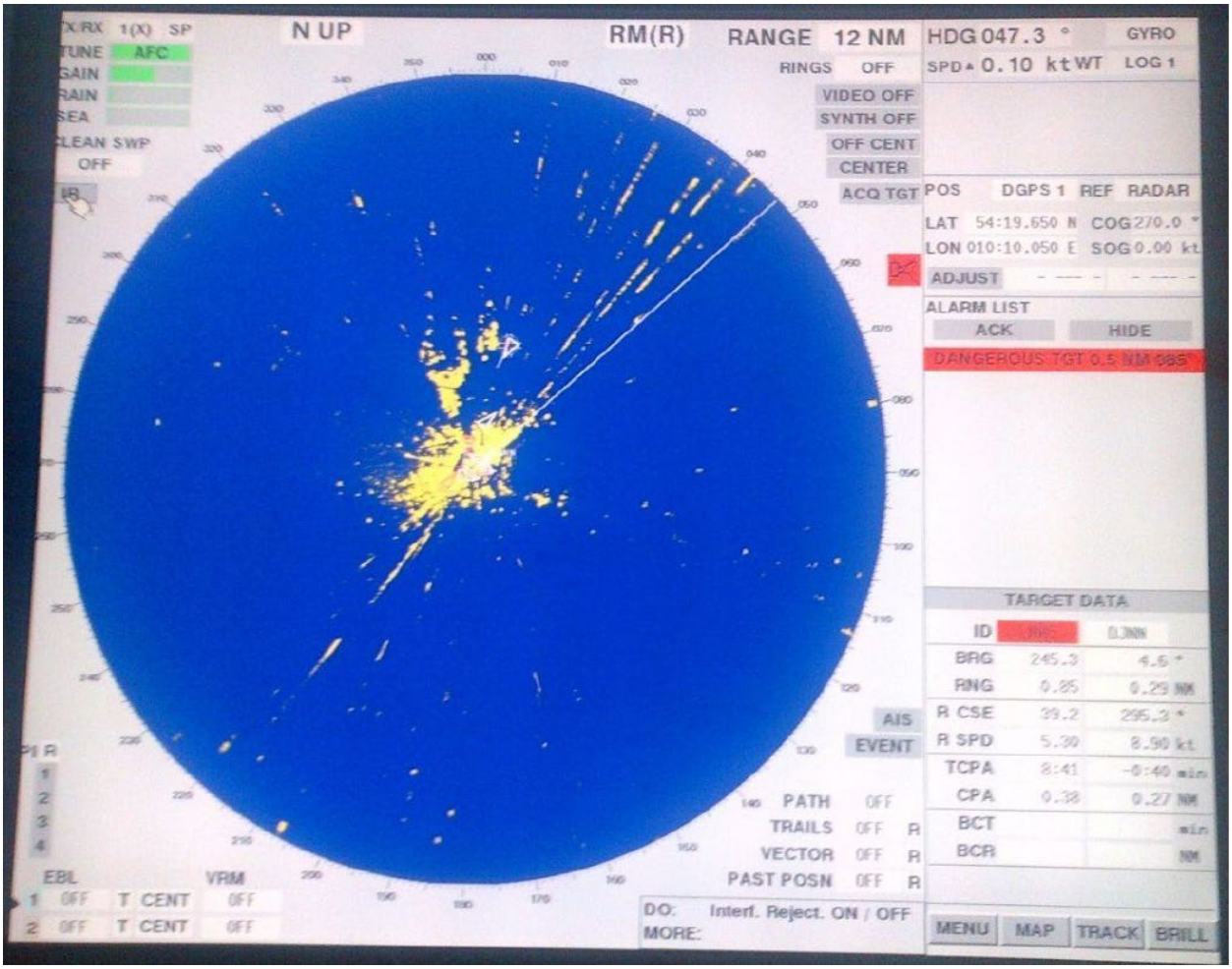

Figure 5. PPI-4, distance separation effect. Radar interference is evident as radials with long dashes centered on 30 and 220 degrees and sparsely dotted spirals centered around 90 and 315 degrees.

3. MODEL

M-MR characteristics are taken from the IEC 62388 shipborne radar standard [10] and three SS-MR signal characteristics are taken from published literature [11],[12],[13]. Since IPC measurements are typically performed in the absence of clutter, M-MR clutter mitigation functions such as fast time constant (FTC), sensitivity time constant (STC), scan to scan correlation, and tracking are not modeled.

3.1 M-MR

A basic block diagram of the M-MR model is provided in Figure 6. For this report, the most important block is the signal processor block which is often referred to as a double threshold detector because it has both analog and digital threshold detection. Characteristics of the signal processing components are summarized in Table 2.

The analog signal processing components include a detection filter, video detector, and video threshold detector. The detection filter impulse response is matched to the pulse. A square law video detector is used. The output of the video threshold detector is either a one or zero depending upon whether the video equals or exceeds the manually set video threshold.

The digital signal processing components include the IR and M out of N (M/N) detector. The IR signal processing component is a PRF discriminator composed of a delay and logical AND gate as shown in Figure 7. The output is set to one if the current and delayed inputs are both ones. Otherwise, it is set to zero. Since the delay is the magnetron radar's own pulse repetition interval (PRI) it will ideally reject signals from other radars with different PRFs. False alarms occur only if the noise or interference plus noise exceed the video threshold for two consecutive PRI.

The M/N threshold detector, sometimes referred to as a binary integrator, continuously counts the number of video detections. Its output is set to one if there are at least M video detections in the last N PRIs. The optimal M/N ratio varies with N [14].

The M-MR transmits three different CW pulses used for short, medium, and long range target detection. The pulses have extremely low duty-cycles and can be approximately modeled with a rectangular shape. In this model, the receiver detection filter impulse response is matched to this pulse shape. However it is important to note that in some M-MR the short range detection filter is used for medium range operation. Table 3 summarizes the relevant pulse characteristics. Table 4 provides parameters for the M/N threshold detector for each of the pulses.

Table 5 summarizes the practical operating, minimum measurement, and maximum unambiguous ranges. The practical operating range is the range suggested by equipment manufacturers for nominal transmit power, the minimum measurement range is

$$r_{min} = \frac{c(\tau - T_{switch})}{2} \tag{1}$$

and the maximum unambiguous range is

$$r_{max} = \frac{c(T_{pri} - \tau)}{2} \tag{2}$$

where c is the speed of light, τ is the pulse width, T_{switch} is the time it takes to switch from transmit to receive, and T_{pri} is the PRI.

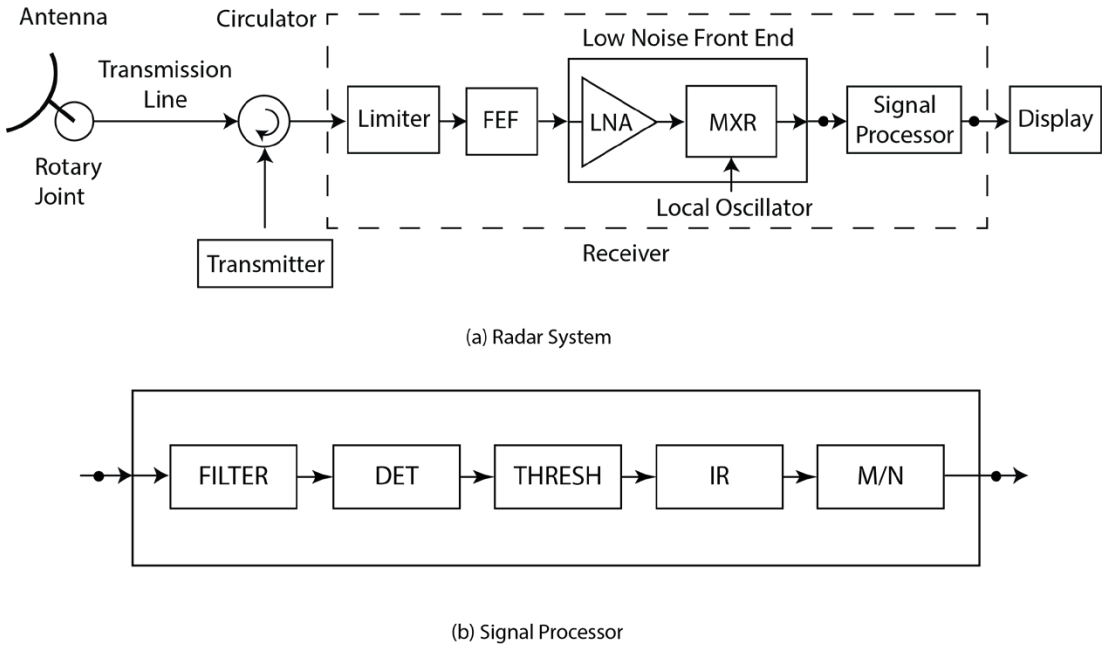

Figure 6. M-MR radar system (a) and signal processor (b). In the radar system FEF represents front end filter, LNA represents low noise amplifier, and MXR represents mixer. In the signal processor DET represents video detector, THRESH represents video threshold detector, IR represents interference rejection, and M/N represent M/N threshold detector.

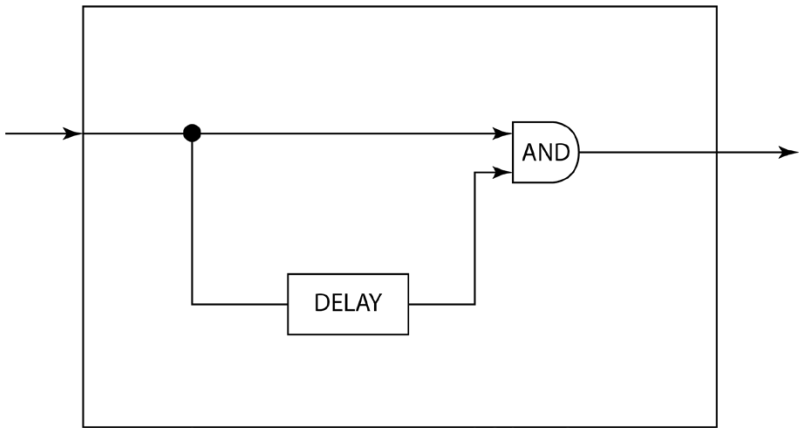

Figure 7. M-MR receiver IR function.

Table 2. M-MR signal processing components.

Component	Note
Detection Filter	Impulse response matched to pulse shape
Video Detector	Square Law
Video Threshold Detector	Manually set
Interference rejection	PRF discrimination
Integration	Binary integration or M/N threshold detection

Table 3. M-MR pulse waveforms. Range gate duration is equal to the pulse width.

Range	Pulse width (ns)	Pulse repetition frequency (Hz)	Duty Cycle	Pulse repetition interval (μs)	Range Gates
Short	50	1800	0.00009	555.5	11,111.1
Medium	250	1800	0.00045	555.5	2,222.2
Long	800	785	0.00063	1273.8	1,592.3

Table 4. Number of pulses in antenna 1.9 degree azimuth beam width and M/N threshold detector parameters for 20 and 40 rpm antenna rotation rates.

	20 RPM			**40 RPM**		
Range	Pulses N	Optimal M/N	Practical M	Pulses N	Optimal M/N	Practical M
Short	29	0.43	13	14	0.51	7
Medium	29	0.43	13	14	0.51	7
Long	12	0.53	6	6	0.60	4

Table 5. M-MR Ranges

Range	Practical Operating Range (NM)	Practical Operating Range (km)	Minimum Measurement Range (NM)	Minimum Measurement Range (km)	Maximum Unambiguous Range (NM)	Maximum Unambiguous Range (km)
Short	3	5.6	0.004	0.0075	44.9	83.3
Medium	0.75-12	1.4-22.2	0.020	0.0375	44.9	83.3
Long	3-24	5.6-44.0	0.064	0.120	107.9	199.8

3.2 SS-MR Signals

Pulsed FM radars that determine target range from the received pulse delay time are typically used for ship navigation. They are sometimes referred to as pulse compression radars because the receiver filter compresses the long FM pulse with poor range resolution into a short baseband pulse with good range resolution. The compression ratio is

$$\gamma = \frac{T}{\tau} = BT \tag{3}$$

where T is the pulse width in time before compression, B is the bandwidth in frequency, and τ is the pulse width in time after compression or 'resolution'.

Pulsed FM SS-MR use signals with three distinct pulses that detect targets at short, medium, and long ranges within the same composite signal PRI. The operator does not have to switch between ranges. The medium and long range pulses use non-linear FM (NLFM) with large compression ratios. The short range pulse cannot achieve a sufficiently large compression ratio and is usually not frequency modulated.

The NLFM pulse match filtered response range side-lobe suppression is determined by its squared spectrum [15] which is shaped by a Taylor window. Frequency offsetting can increase range side-lobe suppression.

FMCW SS-MR are typically used for border security surveillance. FMCW SS-MR modulate the instantaneous frequency with either a saw tooth or triangle waveform. Target range is inferred from the received instantaneous frequency which predictably varies with time. Because of the extremely narrow bandwidths used to detect the instantaneous frequency, FMCW SS-MR can be operated with very little power. The FMCW signal must be switched to detect targets at different ranges.

Two pulsed FM SS-MRs and one FMCW SS-MR derived from published literature were used. Characteristics of the two pulsed FM SS-MR referred to as pulsed FM (Nelander) [11] and pulsed FM (Harman) [12] are summarized in Tables 6 and 7. Short range pulses were modeled as pulsed CW. Medium and long range pulses were modeled with Taylor weighted -40 dB range sidelobes. Characteristics of the FMCW radar [13] are summarized in Table 8.

All SS-MR powers are summarized in Table 9. Pulsed FM power is the average power when pulse is on i.e. peak power. FMCW power is average power. While the pulsed FM (Nelander) power was reported at S-Band it should be the same at X-Band if the antenna aperature is adjusted to maintain the same beamwidth. Pulsed FM waveforms are depicted in Figure 8. All SS-MR PSDs are provided in Figures 9–11.

Table 6. Pulsed FM (Nelander) Signal Characteristics. Composite PRF and PRI are 0.8333 kHz and 1.2 ms, respectively. Inter-pulse spacing is time from start of the current pulse to start of the next pulse.

Range	Range (NM)	Range (km)	Pulses	Inter-pulse spacing (μs)	T (μs)	B (MHz)	τ (μs)	BT	Freq Offset (MHz)
Short	0.16-1.94	0.030-3.6	4	37.5	0.200	5.0	0.200	1	0
Medium	0.97-11.3	1.8-21.0	2	150.0	12.0	20.0	0.050	240	0
Long	9.7-51.0	18.0-94.5	1	750.0	120.0	20.0	0.050	2400	0

Table 7. Pulsed FM (Harman) Signal Characteristics. Composite PRF and PRI are 1.329 kHz and 0.752445 ms, respectively. Inter-pulse spacing is time from start of the current pulse to start of the next pulse.

Range	Range (NM)	Range (km)	Pulses	Inter-pulse spacing (μs)	T (μs)	B (MHz)	τ (μs)	BT	Freq Offset (MHz)
Short	0.19-2.42	0.035-4.5	1	30.586	0.233	4.3	0.233	1	0
Medium	0.52-7.50	4.5-13.9	1	131.874	19.44	3.6	0.277714	70	-6.0
Long	7.50-44.8	13.9-83.0	1	590.19	72.02	1.666	0.600166	120	6.0

Table 8. SS-MR FMCW Signal Characteristics

Range	Range (NM)	Range (km)	T (ms)	B (MHz)
Short	0-6	0-11.1	1.0	54.0
Medium	6-12	11.1-22.2	1.0	27.0
Long	12-24	22.2-44.4	1.0	13.5

Table 9. X-band SS-MR Transmit Power

SS-MR	Power (W)
Pulsed FM (Nelander)	200
Pulsed FM (Harman)	71
FMCW	2

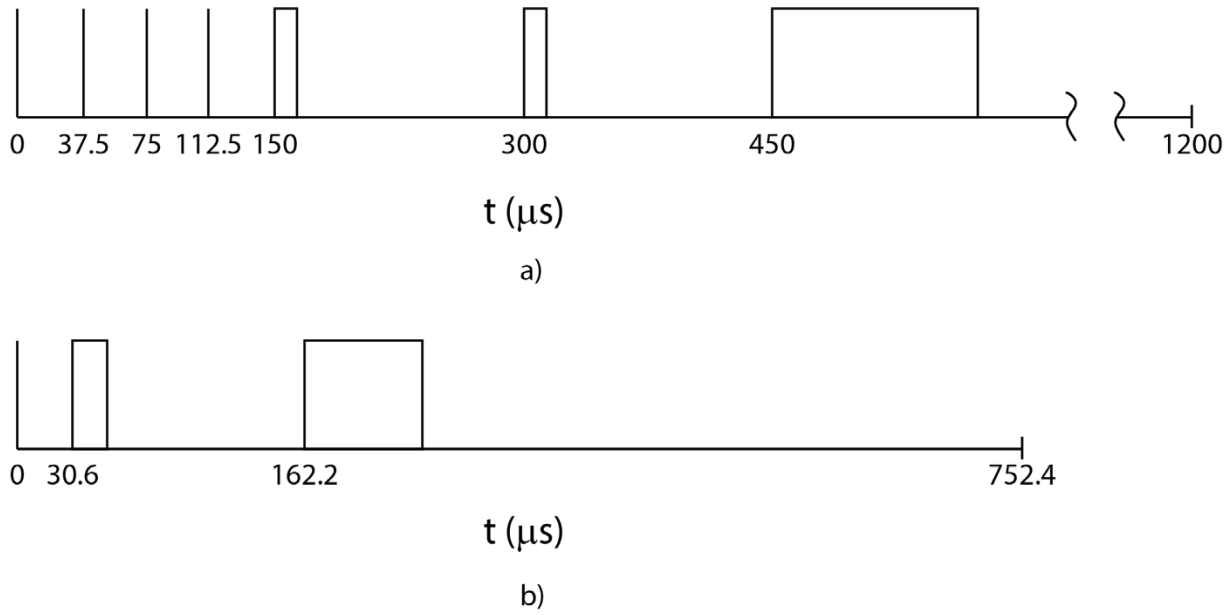

Figure 8. SS-MR signal amplitude over one PRI: a) pulsed FM (Nelander) and b) pulsed FM (Harman).

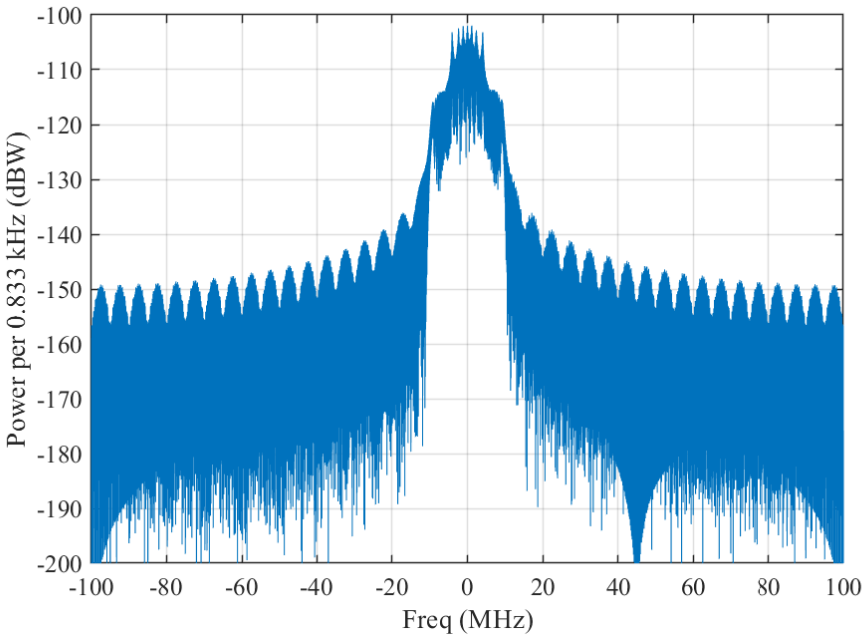

Figure 9. Pulsed FM (Nelander) PSD.

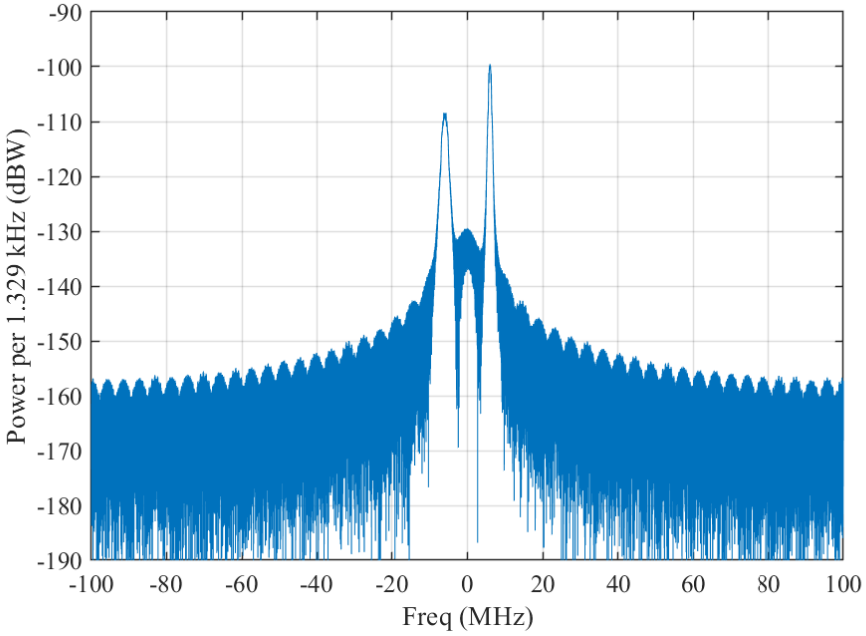

Figure 10. Pulsed FM (Harman) PSD.

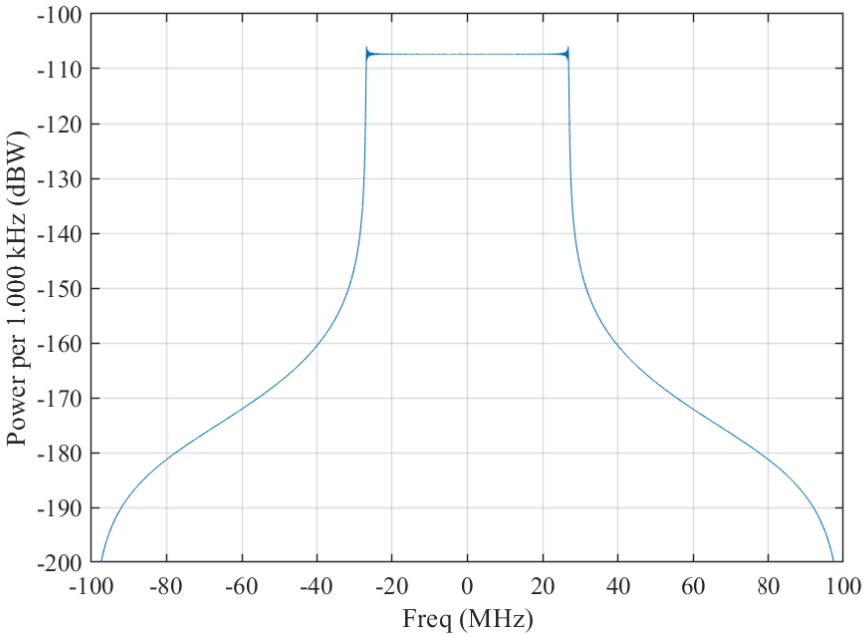

Figure 11. FMCW PSD.

3.3 Antennas

SS-MR and M-MR antennas ([4], Figure 3 curve identified in legend as “Two planar array type antennas with both mainbeams on horizon”) are assumed to be identical and have the

characteristics summarized in Table 10 [17]. The intensity of the interference is dependent on the combined or mutual gain of the two antennas. The mutual antenna gain in decibel units is given by

$$G_m(\theta_t, \theta_r) = G_t(\theta_t) + G_r(\theta_r)\ (dBi) \quad (4)$$

where $G_t$is the SS-MR antenna gain, G_r is the M-MR antenna gain, θ_t is the angular direction from the SS-MR to the M-MR relative to the SS-MR main beam, and θ_r is the angular direction from the M-MR to the SS-MR relative to the M-MR main beam.

Interference analysis is simplified by creating a distribution of mutual antenna gains over all possible angular directions and performing analysis with the gains at a few select percentages of time exceeded, $G_m(\%)$. Figure 12 is a distribution of mutual antenna gains for two antennas similar to those assumed in this report [18].

Simplifying each antenna's gain as either the strong main lobe (ML) or weak side or back lobe (SBL), it is possible to say that the mutual antenna gain between SBLs is weak and frequent, between ML and SBL is moderate and infrequent, and between MLs is strong but rare.

Consequently, the distribution can be divided into 3 distinct regions representing differing kinds of ML and SBL interaction. The concave portion with greater than 5% time exceeded represents weak and frequenct SBL to SBL interaction, the convex portion between 0.5 and 5% time exceeded represents moderate and infrequent ML to SBL interaction, and the straight section above 0.5% time exceeded represents the strong but rare ML to ML interaction.

The mutual antenna gains used for analysis, summarized in Table 11, correspond to the 0.5%, 5.0% , and 50% time exceeded representing ML to SBL, SBL to SBL, and median interactions.

Table 10. Antenna Characteristics

Parameter	**Value**	**Note**
Type	Slotted array	
Frequency range	9200 – 9500 MHz	Marine radar X-band
Length	1.2 meters (4.0 feet)	
Azimuth beam width	1.8 degrees	3-dB beam width
Elevation beam width	24.0 degrees	3-dB beam width
Main lobe gain	28.0 dBi	
First side lobe gain	3.0 dBi	

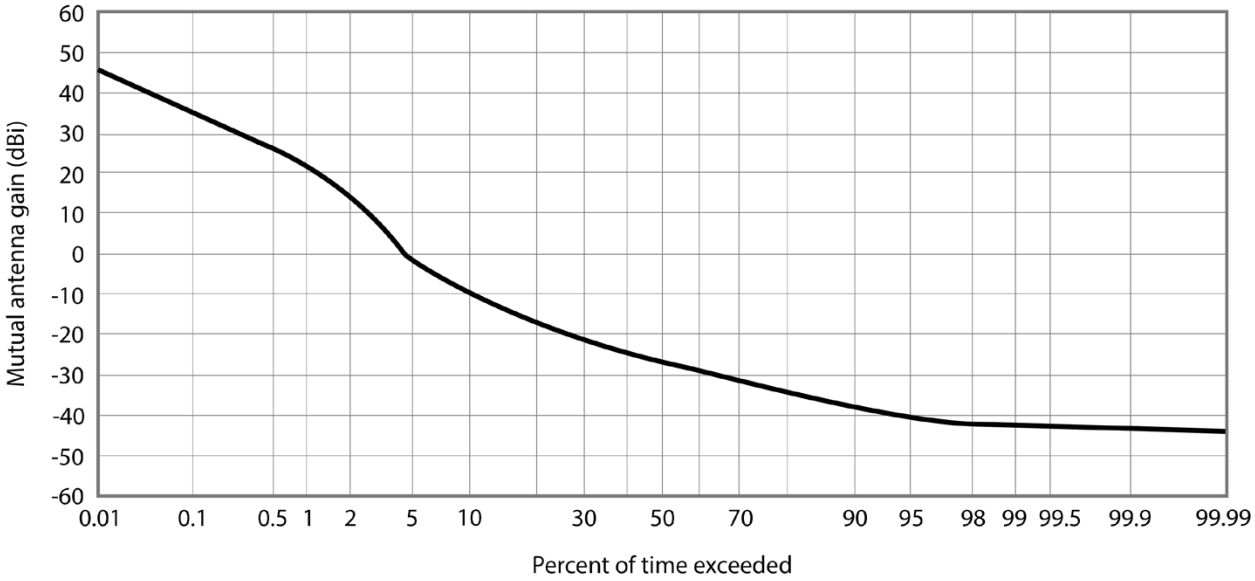

Figure 12. Mutual antenna gain distribution.

Table 11. Mutual antenna gains used for analysis

% of time exceeded	Mutual Gain (dBi)	Interaction
0.5	28.0	ML to SBL
5.0	2.0	SBL to SBL
50.0	-25	Median

3.4 Power and Interference Link Power Budget

The relevant signal powers, defined in Table 12, are all referred to the receiving antenna output which is assumed to be the same point as the receiver input.

Table 12. Signal powers

Signal	Variable	Power Statistic	Note
M-MR signal	s	Peak	
M-MR noise	n	Average	In the detection filter bandwidth but referred to the receiver input
SS-MR pulsed-FM	i	Peak	
SS-MR FMCW	i	Average	Average = Peak

The interference link power budget in decibel units is

$$INR = I_t + G_m(\%) - L_p(d) - N\ (dB) \tag{5}$$

where INR is the received interfering signal power to M-MR noise ratio, I_t is the transmitted interference power at the input to the SS-MR transmit antenna, $G_m(\%)$ is the mutual antenna gain relative to an isotropic antenna at a specified percent of time exceeded, $L_p(d)$ is the free space path loss, d is the distance separation between the interfering and victim antennas, and N is the M-MR receiver noise power.

The free space path loss in decibel units is

$$L_p(d) = 10\log_{10}\left(\frac{4\pi d}{\lambda}\right)^2 \ (dB) \tag{6}$$

where λ is the wavelength of the interfering signal carrier. Finally, the M-MR noise power in decibel units is

$$N = 10\log_{10}(kTbf_{noise}) \ (dB) \tag{7}$$

where k is Boltzman's constant, T is ambient temperature in K, b is the M-MR noise equivalent bandwidth in Hz, and f_{noise} is the M-MR noise factor referred to the receiver input. A 5 dB M-MR receiver noise figure was assumed.

4. METHOD

The method has two parts. The first part uses a commercial radio system software simulation tool to obtain the M-MR IPC against SS-MR signals. The second part uses the interference link power budget analysis to determine the MSD needed to meet the IPC.

4.1 IPC Simulation

The IPC simulation method is based on a radar equipment IPC measurement method developed by the ITS [1] and later adapted to simulation [19]. With this method, radar receiver settings such as the analog video threshold and M-MR signal power are determined for baseline performance in the absence of interference. MR baseline performance is nominally 10^{-4} Pfa and 0.8 Pd. These baseline settings are maintained during IPC simulation where changes in performance are measured as interference power is increased.

The general IPC simulation model block diagram is shown in Figure 13. The lower Pd branch has the victim signal, interfering signal, and receiver noise present. The upper Pfa branch has only the interfering signal and receiver noise. In general, the propagation channels provide only attenuation to control interfering and victim signal powers. The victim propagation channel includes the target radar cross section effects. The signal processor is the double threshold detector described previously.

The victim signal is a series of pulsed CW target returns repeating every PRI so Pd performance measurement samples can be collected every PRI. Pfa is measured in the absence of the target returns so performance measurement samples can be collected every pulse width.

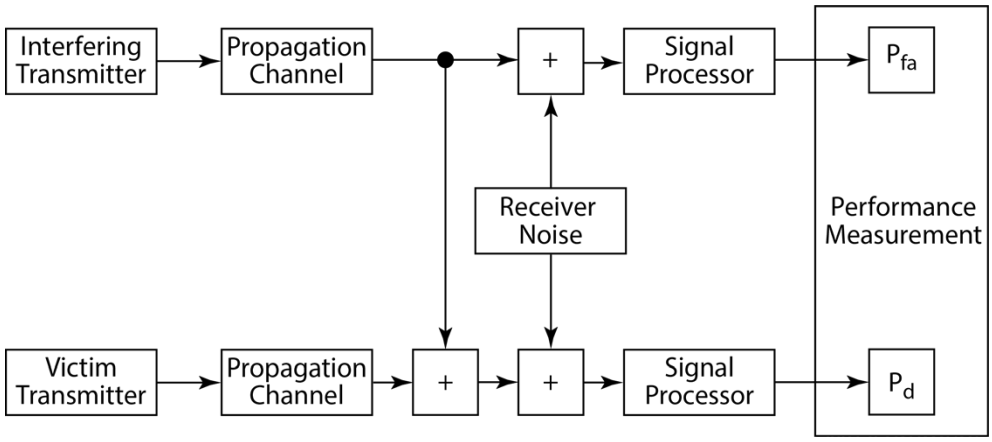

Figure 13 General IPC simulation model.

The IPC simulation method can be summarized in the following six steps:

1) With the victim and interfering signals off, set victim receiver threshold corresponding to baseline Pfa.

2) With the victim signal on and interfering signal off, set the victim SNR corresponding to baseline Pd.

3) Set interfering signal power to the lowest power of interest.

4) With victim and interfering signals on, collect Pd and Pfa performance measurement samples.

5) Incrementally increase interfering signal power and repeat step 4 to the highest interfering signal power of interest.

6) Repeat steps 4 and 5 at other frequency offsets if needed.

These Pfa and Pd versus INR data are analyzed to determine the IPC, defined as the INR needed to drive the Pd or Pfa outside of the baseline confidence interval [7].

4.2 Minimum Separation Distance Analysis

The MSD is the distance between the SS-MR and the M-MR needed to meet the IPC. Separation distances less than the MSD will cause measurable interference in the M-MR. The MSD analysis method begins by replacing the link power budget INR (5) with the IPC and rearranging terms to solve for path loss in decibel units

$$L_p = I_t + G_m(\%) - IPC - N\ (dB) \tag{8}$$

Next the free space path loss equation is rearranged to solve for MSD

$$MSD = \sqrt{l_p}\frac{\lambda}{4\pi} \tag{9}$$

where $l_p = 10^{L_p/10}$.

4.3 Problems Encountered

The principal problem encountered when developing the method was minimizing the IPC simulation computational burden caused by the relatively infrequent coincidences of the asynchronous pulses and the wide simulation bandwidths required by the signals and their frequency separation. A secondary but no less significant problem was the manner with which the baseline condition, i.e. performance in the absence of interference, was set. These problems and their solutions are described below.

4.3.1 Asynchronous Pulse Trains

Pulse trains with different periods are referred to as asynchronous pulse trains. Two characteristics of asynchronous pulse trains, fractional coincidence and asynchronous period are of concern when estimating IPC for radar to radar interference.

Fractional coincidence is the fraction of time pulses of the two pulse trains overlap. Low fractional coincidences impose a computational burden by increasing the simulation time needed to obtain a sufficient number of pulse overlaps for estimating effects of the interference signal on Pd. For Pd estimates an interference event is any amount of pulse overlap. This computational burden is minimized by determining the exact number of Monte Carlo simulation trials needed to obtain the desired estimation uncertainty.

Asynchronous period is the time it takes for the pulse trains to resynchronize. Extremely long asynchronous periods preclude inclusion of all possible interference events. The advantage of a long asynchronous period is the large number of unique interactions possible. If the practical simulation period is shorter than the asynchronous period it is prudent to investigate the diverseness of the events.

Details regarding uncertainty, fractional coincidence, and asynchronous period analysis are summarized in Appendix C.

In the past [1], radar IPC estimation uncertainty has been determined by the number of independent Pd trials, $N_{Pd,ind}$, which ranged from 200 to 500. Since we are analyzing both Pd and Pfa in this work we will continue with this approach.

Uncertainty is expressed in terms of the confidence interval which is strongly influenced by trial correlation. Generally speaking, correlation increases the number of trials needed. In this case, trial correlation is introduced by M/N threshold detection.

For continuous interference the number of Pd trials needed with trial correlation is increased to

$$N_{Pd} = N_{Pd,ind}N \tag{10}$$

where N is the M/N threshold detector window length. The corresponding number of Pfa trials is

$$N_{Pfa} = N_{Pd}N_{rg} \tag{11}$$

where N_{rg} is the number of range gates or pulse widths within one M-MR PRI. Finally, the number of independent Pfa trials is

$$N_{Pfa,ind} = \frac{N_{Pfa}}{N} = N_{rg}N_{Pd,ind} \tag{12}$$

Neglecting effects of receiver filtering, asynchronous pulsed interference can only influence Pd when the SS-MR pulses overlap M-MR pulses. Without trial correlation, the number of Pd trials needed can be estimated with the analytic fractional coincidence. With Pd trial correlation, we must simulate.

The simulation is performed in the absence of noise and frequency separation. A Pd independent interference event occurs when there is a least one overlap in a block of N distinct and contiguous M-MR pulses. The actual number of Pd trials, N_{Pd}, is the number of trials needed to have $N_{Pd,ind}$ independent interference events. The corresponding N_{Pfa} and $N_{Pfa,ind}$ can be determined by (11) and (12), respectively.

The actual numbers of Pd trials are provided in Table 13. A 40 rpm antenna rotation rate is used to minimize the number of integrations. Pd 95.5% (2-sigma) confidence intervals for 200 independent trials ranged from 0.7364 to 0.8540 for 0.8 Pd. Corresponding Pfa results for 10^{-4} Pfa are provided in Table 14.

All pulsed FM interference simulation times are less than the asynchronous periods. Further tests investigated how diverse the interference events in the shorter simulation time were. These tests showed that the interference events were caused by all the SS-MR signal pulses – short, medium, and long and the frequency with which the pulses caused interference events was proportional to the SS-MR pulse width. Consequently, we concluded the use of a shorter simulation time was representative of the interference that would have occurred had we simulated the entire asynchronous period.

Table 13. Pd Trials, Pfa trials, and simulation time needed for 200 independent Pd interference events for a 40 rpm antenna rotation rate. Asynchronous are computed with 10 ns resolution.

	Actual Pd trials N_{Pd}	**Actual Pfa trials N_{Pfa}**	**Simulation time (s)**	**Asynchronous Period (s)**
Pulsed FM (Nelander)				
Short	2800	31,110,800	1.555	16.66
Medium	2800	6,221,600	1.555	16.666
Long	2496	3,973,632	3.179	50.95
Pulsed FM (Harman)				
Short	3108	34,532,988	1.726	41.80
Medium	3108	6,905,976	1.726	41.80
Long	2166	3,448,272	2.759	95.85
Continuous				
Short	2800	31,110,800	1.555	NA
Medium	2800	6,221,600	1.555	NA
Long	1200	1,910,400	1.528	NA

Table 14. Pfa independent trials and 95.5 % confidence interval for 10^{-4} Pfa.

Magnetron Pulse	Independent Pfa trials $N_{Pfa,ind}$	Pfa confidence interval (x10^{-4})
Pulsed FM (Nelander)		
Short	2.2220e6	0.8703 to 1.143
Medium	0.4444e6	0.7230 to 1.347
Long	0.6622e6	0.7696 to 1.277
Pulsed FM (Harman)		
Short	2.4666e6	0.8767 to 1.135
Medium	0.4932e6	0.7359 to 1.327
Long	0.5747e6	0.7539 to 1.300
Continuous		
Short	2.222e6	0.8703 to 1.143
Medium	0.4444e6	0.7230 to 1.347
Long	0.3184e6	0.6778 to 1.421

4.3.2 Simulation Bandwidth

The full simulation bandwidth needed to accommodate the M-MR signal bandwidth, SS-MR signal bandwidth, and frequency separation between them can unduly burden simulation execution time. Our approach to minimizing the simulation bandwidth is to preprocess the SS-MR signal so only the portion in the bandwidth needed to accurately simulate the M-MR is used.

Preprocessing consists of simulating the SS-MR signal in a bandwidth, BW_{ss}, greater than or equal to the full bandwidth, BW_{full}, applying the frequency shift, Δf, and resampling to the M-MR simulation bandwidth, BW_m. The preprocessed SS-MR signal is stored in a file that is played back during the IPC simulation. A gain block in the IPC simulation adjusts the SS-MR signal power to the desired INR. This process is summarized in Figure 14.

Figure 14. Simulation bandwidth minimization process.

The full simulation bandwidth is

$$BW_{full} = 2\left(\frac{BW_m}{2} + |\Delta f|\right) \tag{13}$$

and the SS-MR simulation bandwidth must satisfy

$$BW_{ss} \geq BW_{full} \tag{14}$$

to avoid aliasing.

Table 15 shows how this was done for IPC simulations for each of the M-MR pulses. For example, for the short M-MR pulse, BW_m is 200 MHz, Δf is 55 MHz, and BW_{full} is 310 MHz. BW_{ss} is rounded up to 400 MHz so it can be simply resampled by a factor of 2 to return to the BW_m.

The SS-MR signal is generated at 1 volt peak into the reference impedence R_{ref}. Although its power is reduced by the frequency shifting and resampling, this reduction is not compensated for so it is as if its full power is present at the victim receiver input. During IPC simulation the gain block scales the SS-MR power by

$$g_i = \sqrt{\frac{inr \cdot n}{1^2/R_{ref}}} \tag{15}$$

to achieve the desired INR.

Table 15. Simulation bandwidths

Magnetron Pulse	M-MR Simulation Bandwidth (MHz)	Frequency Separation (MHz)	Full Bandwidth (MHz)	SS-MR Simulation Bandwidth (MHz)	Resample Ratio
Short	200	55	310	400	2
	200	135	470	800	4
Medium	40	55	150	400	10
	40	135	310	400	10
Long	12.5	55	122.5	400	4,8 = 32
	12.5	135	282.5	400	4,8=32

4.3.3 Baseline Conditions

Setting the baseline condition is complicated by the M-MR signal processor having a manual threshold and IR. The threshold is higher with IR off than when IR is on for the same Pfa. If the baseline Pfa and Pd are set with IR off, false alarms and detections are significantly decreased making IPC estimation difficult with IR on. If baseline Pfa and Pd are set with IR on, false alarms and detections are significantly increased making IPC estimation difficult with IR off.

Consequently, assuming that the threshold was not changed between frequency separation, IR, and distance separation field tests, we used a “mixed mode” that set the baseline Pfa (i.e. set the threshold) with IR off and baseline Pd (i.e. set the SNR) with IR on.

Table 16 shows results of tests using the magnetron short pulse for all three modes i.e. baseline Pd and Pfa set with IR off, Pd and Pfa set with IR on, and the mixed mode. The results were collected at the output of the video threshold detector, at output of the M/N threshold detector with IR off, and at output of the M/N threshold detector with IR on. Test conditions include a 0 dB noise figure, 40 rpm antenna rotation rate, and 1.9 degree beamwidth. Baseline conditions for mixed mode for all magnetron pulses are provided in Table 17.

Additional tests using the magnetron short pulse were conducted to show how these different approaches to setting baseline might affect the IPC measurement. Although Pd and Pfa could differ dramatically between approaches these differences occurred at INR far greater than the IPC. Hence it was concluded that using mixed mode did not compromise IPC estimation.

Table 16. Baseline test results for short range mangnetron pulse for various combinations of video thresholds and SNR. Shaded values represent target baseline conditions.

Mode	Baseline IR	Video Threshold (v^2)	SNR (dB)	Video Pd	Video Pfa	M/N IR off Pd	M/N IR off Pfa	M/N IR on Pd	M/N IR on Pfa
1	Off	$9.55x10^{-12}$	3.7	0.59	0.085	0.801	$1.13x10^{-4}$	0.165	0
2	On	$4.77x10^{-12}$	2.84	0.753	0.289	0.99	0.095	0.800	$0.94x10^{-4}$
3-mixed	Off	$9.55x10^{-12}$	5.5	0.756	0.098	0.993	$1.05x10^{-4}$	0.787	0

Table 17. Baseline test results for mixed mode. Shaded values represent target baseline conditions.

Magnetron Pulse	Video Threshold (v^2)	SNR (dB)	Video Pd	Video Pfa	M/N IR off Pd	M/N IR off Pfa	M/N IR on Pd	M/N IR on Pfa
Short	$9.55x10^{-12}$	5.5	0.756	0.098	0.993	$1.05x10^{-4}$	0.787	0
Medium	$1.89x10^{-12}$	5.5	0.733	0.087	0.993	$0.91x10^{-4}$	0.807	0
Long	$1.01x10^{-12}$	7.65	0.758	0.019	0.973	$1.06x10^{-4}$	0.805	0

5. RESULTS

Three types of results are presented in this section. The first, IPC simulation results, determine the maximum interference power tolerated by the M-MR receiver. The second, MSD results, use the IPC and the interference link power budget to determine how far away the SS-MR must be from the M-MR to mitigate interference. The third, field test comparison results, use the IPC and the interference link power budget to qualitatively predict the interference seen in the field test.

5.1 IPC Simulation Results

The IPC simulations were completed for short, medium, and long range M-MR operation, IR on and off, 55 and 135 MHz frequency separation, INR ranging from 0 to 150 dB in 5 dB increments. A 40 rpm antenna rotation rate was used.

Results for the 55 MHz frequency separation are shown in Figures 15–17. All the graphs show Pfa and Pd increasing with INR which is characteristic of radars with constant video thresholds. Corresponding results for the 135 MHz frequency separation are not shown because its IPC were at a minimum on the order of 70 dB greater than that of the 55 MHz frequency separation.

Recall that the IPC is the INR needed to drive the Pd or Pfa outside of the baseline confidence interval. IPC corresponding to results in Figures 15–17 are shown in Table 18. IPC was lowest for the M-MR short range. M-MR medium and long range IPC were significantly higher than that for the short range. The Pfa IPC occur at lower INR than the Pd IPC for all M-MR ranges. Consequently the Pfa case is considered to be the limiting case.

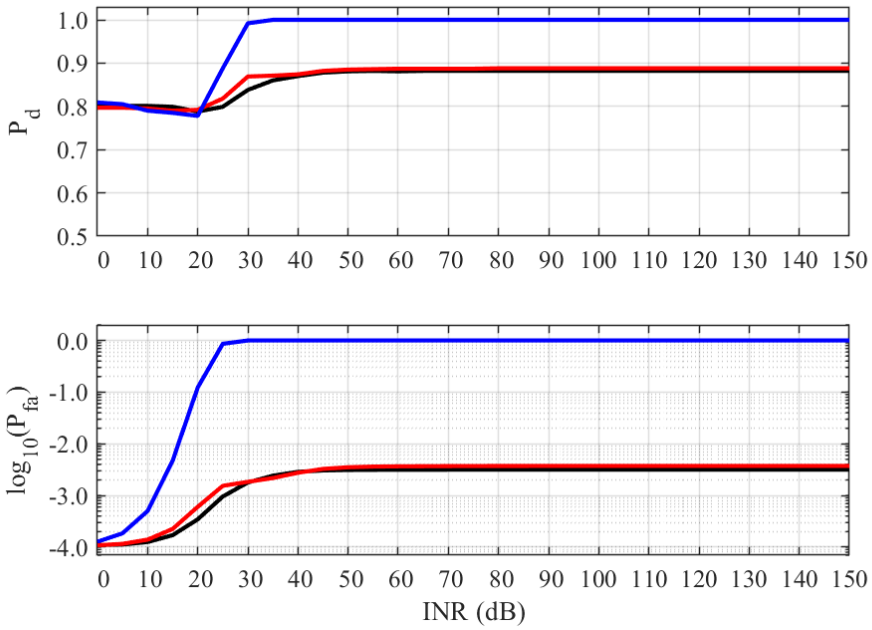

Figure 15. Short range magnetron pulse results. Black is pulsed FM (Nelander), red is pulsed FM (Harman), and blue is FMCW. Pfa and Pd have IR off and on, respectively.

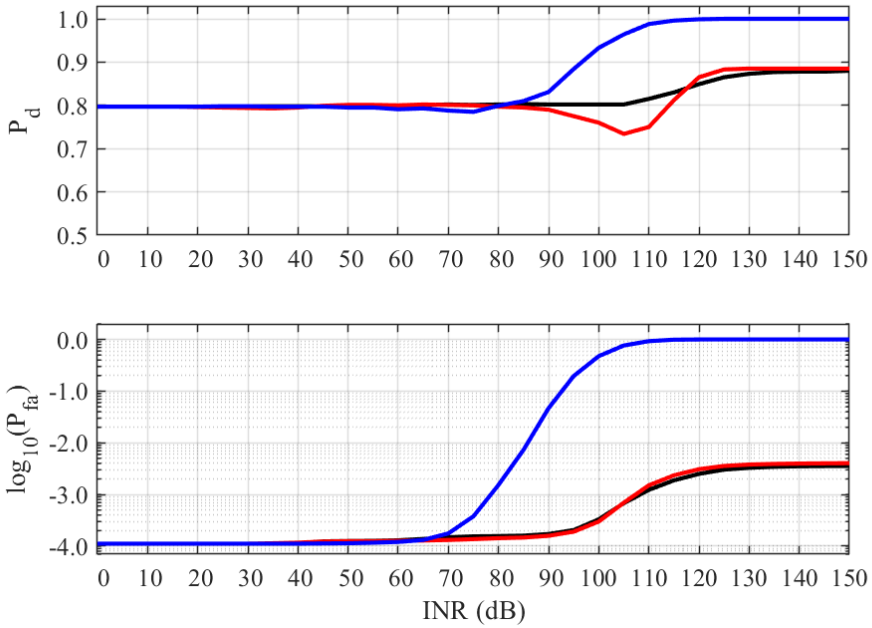

Figure 16. Medium range magnetron pulse results. Black is pulsed FM (Nelander), red is pulsed FM (Harman), and blue is FMCW. Pfa and Pd have IR off and on, respectively.

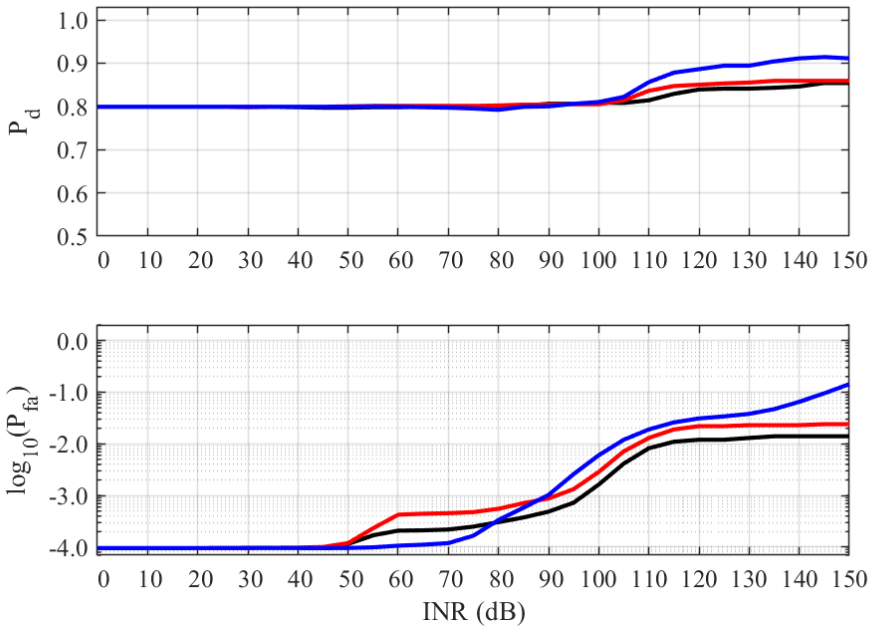

Figure 17. Long range magnetron pulse results. Black is pulsed FM (Nelander), red is pulsed FM (Harman), and blue is FMCW. Pfa and Pd have IR off and on, respectively.

Table 18. IPC results at 55 MHz frequency separation.

M-MR Range	SS-MR Signal	IPC (dB) Pfa (without IR)	IPC (dB) Pd (with IR)
Short	Pulsed FM (Nelander)	10	35
	Pulsed FM (Harman)	5	30
	FMCW	0	25
Medium	Pulsed FM (Nelander)	65	125
	Pulsed FM (Harman)	75	105
	FMCW	70	95
Long	Pulsed FM (Nelander)	55	144
	Pulsed FM (Harman)	55	130
	FMCW	75	110

5.2 Minimum Separation Distance Analysis Results

MSD results are summarized in Table 19. These results show that short range operation is the most vulnerable since it is the only range with a significant 50% MSD and the 5% and 0.5% MSD are not practical to acheive. Medium and long range 5% and 0.5% MSD are considerably less than that of short range. Still, some of these may also be inpractical to achieve.

The two pulsed FM MSDs are comparable and greater than FMCW MSDs. Consequently the pulsed FM signals are more detrimental to the M-MR than the FMCW signal. This is an interesting result for the short range since the pulsed FM signals had higher IPC than the FMCW. While high IPC is indicative of less interference potential, when transmitted power is factored in to compute the MSD the pulsed FM signals showed greater interference potential.

Table 19. Separation distance results at 55 MHz frequency separation. Not applicable (NA) values are below the minimum measurement range. Shaded values are the greatest for that M-MR range and % of time exceeded.

		MSD (NM) Pfa without IR		
		% of time exceeded		
M-MR Range	**SS-MR Signal**	50.0%	5.0%	0.5%
Short	Pulsed FM (Nelander)	0.69	15.46	308.61
	Pulsed FM (Harman)	0.73	16.39	326.98
	FMCW	0.22	4.89	97.59
Medium	Pulsed FM (Nelander)	NA	0.06	1.23
	Pulsed FM (Harman)	NA	NA	0.23

M-MR Range	SS-MR Signal	MSD (NM) Pfa without IR		
		% of time exceeded		
		50.0%	5.0%	0.5%
	FMCW	NA	NA	0.07
Long	Pulsed FM (Nelander)	NA	0.35	6.94
	Pulsed FM (Harman)	NA	0.21	4.14
	FMCW	NA	NA	0.07

5.3 Comparison to Field Test Results

Field tests evaluated how well frequency separation, IR, and distance separation mitigated SS-MR interference by comparing the PPI interference in Figures 2–5. Besides a rain event no known target was present. Consequently, only effects on false alarms are evaluated. These false alarms, collectively manifested as dashed radials and running rabits, are assumed to occur whenever the interference exceeds the IPC.

The PPI ranges of 6 to 12 NM suggests operation in the medium range. Interestingly, the only simulation results that showed the significant interference interference in PPI-2, i.e. 50th percentile interference, were for the short range. One explanation for this discrepancy may be that the field test M-MR used the short range bandwidth for medium range operation as is sometimes done. To proceed, we assume this was the case and compare the field test PPI presumably acquired in medium range operation to simulation results in short range operation.

As noted previously frequency separation simulation and analysis results showed almost complete elimination of false alarms. This is somewhat in agreement with the frequency offset field test PPI-1 that showed SS-MR false alarm interference significantly reduced but not completely eliminated. This small discrepancy may be due to the simulation not modeling the SS-MR amplifier's non-linear behavior.

Also, as noted previously, IR simulation and analysis results showed almost complete elimination of false alarms. This is also somewhat in agreement with the IR field test PPI-3 which showed SS-MR false alarm interference mitigated but not completely eliminated. This discrepancy may be due to the particular combination of IR and SS-MR signals used.

Distance separation results are evaluated by comparing INR to IPC at the two different field test distances as is done in Table 20. The results show that the 50% INR exceeds IPC at 0.34 NM but not at 2.0 NM. These results compare favorably to the reference PPI-2 at 0.34 NM with significant false alarms and the distance separation test PPI-4 with significantly fewer.

Hence, for the M-MR and SS-MR characteristics assumed, the frequency separation, IR, and distance separation results seem to correlate with those of the field test.

Table 20. Field test emulation results for short range M-MR operation at two separation distances. Frequency separation is 55 MHz frequency separation and IR is off. Shaded values exceed IPC and have potential for interference.

SS-MR Signal	Sep. Dist. (NM)	IPC (dB)	INR (dB)		
			% of time exceeded		
			50%	5.0%	0.5%
Pulsed FM (Nelander)	0.34	10	16.2	43.2	69.2
Pulsed FM (Harman)	0.34	5	11.7	38.7	64.7
FMCW	0.34	0	-3.8	23.2	49.2
Pulsed FM (Nelander)	2.00	10	0.8	27.8	53.8
Pulsed FM (Harman)	2.00	5	-3.7	23.3	49.3
FMCW	2.00	0	-19.2	7.8	33.8

6. CONCLUSION

This report describes a method that can be used to evaluate SS-MR interference in M-MR. It then uses the method to evaluate SS-MR interference from three SS-MR signals – two pulsed FM and one FMCW - into an M-MR. Finally, it uses the method to evaluate previously published field test results that anecdotally demonstrated SS-MR interference in M-MR.

The method consists of two parts. The first part uses a commercial radio system software simulation tool to model the M-MR radar and emulate a hardware IPC measurement method previously developed by the ITS [1] The second part uses the interference link power budget to determine the MSD needed to meet the IPC. While lower IPC increases interference susceptibility it is only one factor in determining MSD which is of the most concern since long MSDs are often difficult to achieve.

The M-MR receiver model featured double threshold detection, PRI discrimination IR, and short, medium, and long range operational modes. IPC for three SS-MR signals were obtained for each of these modes. MSD were computed at the 50, 5, and 0.5 percentiles of time exceeded based on mutual antenna gain statistics.

The simulations and analysis with IR off and a 55 MHz frequency separation showed that the short range had both the lowest IPC and longest MSDs and therefore was the range most susceptible to SS-MR interference. Short range was also the only range that had significant MSD at the 50 percentile. However, it is worth noting that medium and long range MSD still could be significant at the 5 and 0.5 percentiles.

Simulations and analysis also showed that pulsed FM signals had longer MSD and therefore more interference potential than the FMCW signals at all ranges. Finally, enabling IR and increasing frequency separation from 55 to 135 MHz were both very effective at mitigating the SS-MR interference.

Only short range simulations achieved the high false alarms seen in the field test. Since the field test PPI displays suggested operation in medium range we assumed the field test M-MR radar medium range used a short range bandwidth and its PPI results could be compared to our short range results. Given this and all the other assumed M_MR equipment parameters and SS-MR interfering signal characterisitcs, the simulation and analysis method results seem to support field test results i.e. that IR, frequency separation, and distance separation are fairly effective SS-MR interference mitigation measures.

MRs are not guaranteed interference-free radio spectrum. This is why all M-MR have some sort of IR. Even the simplest PRI discrimination IR used by this method is remarkably effective at removing interference from other M-MRs and these results demonstrated that it is also effective at mitigating interference from a single SS-MR. This finding is important in the event that adequate frequency or distance separations are not available. However, there is a concern that legacy M-MR IR may not be as effective at removing the interference from multiple SS-MRs present in a crowded harbor or port where distance separation is difficult to achieve.

The next logical step for improving this method would be to establish standardized M-MR receiver settings and baseline operating conditions. Analysis also needs to be expanded to include other SS-MR and aggregate SS-MR interfering waveforms.

The numbers and characteristics of new SS-MR signals will inevitably increase with the advances in solid state device and digital signal processing technologies. Some of these new SS-MR signals may have even higher duty cycles than the ones used here. Clearly a method for evaluating the compatibility of these new SS-MR signals is needed. The simulation and analysis method described in this report, which quantifies the maximum interfering signal power and MSD, is a significant first step in this direction.

7. REFERENCES

[1] F. Sanders, R. Sole, B. Bedford, D. Franc, T. Pawlowitz, "Effects of RF Interference on Radar Receivers," NTIA Report TR-06-444, Feb. 2006. Available https://www.its.bldrdoc.gov/publications/2481.aspx

[2] German delegation to the IMO, "Observed interference on marine radar," Joint IMO/ITU Experts Group on Maritime Radio-communication Matters, 11th Meeting, Agenda Item 6, Sept. 25, 2015.

[3] G. Galati, G. Pavan, F. De Palo, "Interference problems expected when solid-state marine radars will come Into widespread use," in *Proc. of Eurocon 2015, International Conference on Computer as a Tool*, Salamanca, Spain, Sept. 8-11, 2015.

[4] Recommendation ITU-R M.1372-1, (2003), *Efficient use of the radio spectrum by radar stations in the radio determination service*, International Telecommunications Union,Geneva, Switzerland.

[5] Report ITU-R M.2076, (2006), "Factors that mitigate interference from radiolocation and Earth exploration-satellite service/space research service (active) radars to maritime and aeronautical radionavigation radars in the 9.0-9.2 and 9.3-9.5 GHz bands and between Earth exploration-satellite service/space research service (active) radars and radiolocation radars in the 9.3-9.5 and 9.8-10.0 GHz bands," International Telecommunications Union, Geneva, Switzerland.

[6] "Defense Against Enemy Countermeasures," Part 3 p 31 in *Radar Operator Manual*, Radar Bulletin No. 3, U.S. Government Printing Office 1945-6388S9.

[7] F. Sanders, "The Rabbit Ears Pulse-Envelope Phenomena in Off-Fundamental Detection of Pulsed Signals," NTIA Technical Report TR-487, July 2012. Available https://www.its.bldrdoc.gov/publications/2678.aspx

[8] International Electrotechnical Commission, "Maritime navigation and radio communications equipment and systems-shipborne radar-performance requirement, methods of testing and required test results," IEC 62388, Edition 1.0, 2007-12

[9] A. Nelander and Z. Tóth-Pál, "Modular System Design for a New S-Band Marine Radar," *IEEE 2009 International Radar Conference "Surveillance for a Safer World (RADAR 2009)*, Bordeaux, Oct. 12-16, 2009, pp 1-5.

[10] S. Harman, "The Performance of a Novel Three-Pulse Radar Waveform for Marine Radar Systems," *2008 European Radar Conference*, Amsterdam, The Netherlands, October 2008, pp 160-163.

[11] S. Plata, R. Wawruch, "CRM-203 Type Frequency Modulated Continuous Wave (FM CW) Radar," *International Journal on Marine Navigation and Safety of Sea Transportation*, Vol. 3, No. 3, Sept. 2009, pp. 311-314

[12] R. Worley, "Optimum Thresholds for Binary Integration," IEEE Trans. on Information Theory, March 1968, pp. 349-353.

[13] *Principles of Modern Radar: Advanced Techniques*, W. Melvin and J. Scheer (editors), Institution of Engineering and Technology, 2014, pp. 48-57.

[14] J. Briggs, "Typical scanner parameters," Table 2.3 in Section 2.7.6 of *Target Detection of Marine Radars*, Institution of Electrical Engineers, London, United Kingdom 2004, p73.

[15] International Electrotechnical Commission, "X-band radar parameters," Table D.9 of "Maritime navigation and radio communications equipment and systems-shipborne radar-performance requirement, methods of testing and required test results," IEC 62388, Edition 1.0, 2007-12

[16] R. J. Achatz and B. Bedford, "Interference protection criteria simulation," NTIA Report TR 19-450, Aug. 2019. Available https://www.its.bldrdoc.gov/publications/3221.aspx

[17] Report ITU-R M.2050, (2003), "Test results illustrating the susceptibility of maritime radio navigation radars to emissions from digital communication and pulsed systems in the bands 2900-3100 and 9200-9500 MHz," International Telecommunications Union, Geneva, Switzerland, Section 6.7.2 Radar B (3GHz).

ACKNOWLEDGEMENTS

This work was sponsored by the U.S. Coast Guard Spectrum Management Telecommunications Policy Division, U.S. Coast Guard CG-652, 2100 2nd St. SW Stop 7101, Washington DC 20593-7101. The authors would like to acknowledge Joseph Heresey (former Division Chief), Jerry Ulcek, Telecommunication Specialist, and Brad Benbow, Electronics Engineer, for their sponsorship.

Finally, the authors would like to acknowledge Al Romero, Visual Information Specialist, at the National Oceanic and Atmospheric Administration (NOAA) for creating the illustrative figures.

APPENDIX A PRIOR ITS RESEARCH ON INTERFERENCE IN MARINE SURVEILLANCE RADARS

Prior ITS research on interference in marine surveillance radars (MSR) [A-1] measured the interference in six MSRs from 1) continuous, noise-like communication signals, 2) pulsed radar signals, and 3) pulsed ultrawideband signals. Desired radar target signals and undesired interfering signals were generated by laboratory equipment and injected into the radar receiver front end (RF assembly composed of preselection filter, low noise amplifier, and frequency downconverter). Performance was evaluated with radar display interference observations. These measurements were also reported in ITU-R Report M.2050 [A-2]. Similar measurements were reported in ITU-R Report M.2032 [A-3].

The research cited three principal mechanisms that were expected to mitigate interference: pulse to pulse correlation, scan to scan correlation, and constant false alarm rate (CFAR) signal processing. Of the three only pulse to pulse correlation, often referred to as the interference rejection (IR), was designed to mitigate interference from other radars. Scan to scan correlation and CFAR are designed to mitigate effects of wave clutter.

IR is designed to mitigate interference between magnetron transmitter tube MSRs with diverse short pulse widths (PW) and pulse repetition intervals (PRI). IR plays a critical role in maximizing the number of MSR that can operate in the crowded conditions found in ports and harbors. It is unclear how well IR works with dissimilar pulsed signals with longer PWs and higher duty cycles and continuous signals.

Scan to scan correlation allows MSRs to favor target detections that persist over multiple antenna rotation periods while deemphasizing random wave clutter detections that do not persist. Scan to scan correlation is expected to be most effective against low duty cycle pulsed signals.

CFAR adaptively sets the detection threshold to accommodate variable wave clutter conditions. CFAR is expected to mitigate false alarms from continuous noise like communication signals while lowering the probability of detecting targets. The effectiveness of CFAR mitigating pulsed interference is expected to depend on the algorithm used to determine the threshold. Radars In these tests used the order statistic algorithm. Continuous and pulsed interfering signals are expected to create false alarms in radars without CFAR. While targets are not expected to disappear from the display in radars without CFAR, they are expected to be more and more obscured as the false alarm density increases. This effect is most noticeable towards the center of the radar display where azimuths are more concentrated.

A.1 MSR Radars, Signals, and Settings

The radars used, listed in Table A-1, operate in either the S band (2900-3100 MHz) or X band (9300-9500 MHz). Paired radars B/D and C/E operate in distinct bands with separate front ends but share receiver signal processing functions and displays. Radars A and F operate in distinct bands with separate front ends, signal processing functions, and displays. However, radars A and F are reported to have nearly identical signal processing functions and displays.

All radars have IR and scan to scan correlation but only radars A and F are reported to have CFAR. All the radars have wide dynamic range log amps and can display "raw" video. In this context "raw" means video without "synthesized" targets discerned by proprietary signal processing algorithms. It does not mean that the signal was completely unprocessed. For example the signals did have IR and scan to scan correlation processing before display.

Table A-1. Interference Mitigation Factors

Radar Designator	Band(s)	CFAR	Notes
A/F	S/X	Yes[4]	Scan to Scan correlation with spike suppression for synthetic targets Order statistic CFAR with clutter map bias for synthetic targets Displays synthesized targets
B/D	S/X	No	Transmitted pulses have jitter to increase effectiveness of IR
C/E	S/X	No	

The MSR signal injected into the radar receiver emulates 10 colinear stationary targets across the radar range. The targets appear as small bright lights spread evenly across a single radar display radial. Except for Radar F, the shortest range was used for each radar (Note: Private communication with report author). Every target was provided enough pulses to satisfy its pulse integration needs within the rotating antenna 3-dB beamwidth. The target powers are constant across the radial, so their radar cross sections are assumed to increase with range to compensate for different propagation losses. Corresponding MSR signal and receiver parameters used for each radar are listed in Table A-2.

Table A-2. MSR parameters.

Radar Designator	Range (nm)	PW	PRF (kHz)	PRI (ms)	Receiver BW (MHz)
A	0.375-1.50	80	2.2	0.45	28.0
F	0.5 to 3.0	200	2.2	0.45	4.5
B/D	1.25-1.50	70	1.55	0.322	22.0
C/E	0.125 to 3.0	50	1.8	0.56	20.0

In addition to the IR and scan to scan correlation functions mentioned, all radars have automatic gain control (AGC), sensitivity time control (STC), and fast time constant (FTC) functions. STC and FTC are specialized MSR functions used to mitigate nearby wave clutter and rain clutter, respectively. STC and FTC were disabled because the test was performed in the absence of nearby wave clutter and rain. The settings of these functions are summarized in Table A-3.

Table A-3. MSR function settings.

Feature	Function	Setting
Interference Rejection	Radar interference mitigation	On

[4] The report mentions that radar A and F false alarms increased with continuous interfering signal power. This result is not typical of a radar with CFAR.

Feature	Function	Setting
Scan to Scan correlation	Wave clutter mitigation	On
Automatic Gain Control	Match receiver dynamic range to signal plus interference powers	On
Sensitivity Time Control (STC)	Nearby clutter mitigation	Off
Fast Time Constant (FTC)	Rain clutter mitigation	Off

A.2 Interfering Signals

Continuous, noise-like signals generated by communications transmitters, pulsed signals generated by radars, and ultrawideband radios were used. Table A-4 lists the interfering signals along with which radar they were used with. The interfering signals were generated cochannel at the radar's center frequency. The term gated means the interference was turned on only when the target signal was present emulating main-beam to main-beam antenna coupling between radars. Gated interference can appear on the radar display as a "strobe" when false alarms rates are high.

The chirped radar signals used with Radar F were modified to accommodate laboratory equipment bandwidth limitations. The laboratory equipment was only capable of frequency sweeping over a 80 MHz range. To emulate linear FM (i.e. chirped) pulses sweeping over ranges greater than 80 MHz the sweep rate was kept constant and the pulse width and frequency range were proportionally truncated. This was believed to be sufficient for cochannel tests provided the radar bandwidth was less than 80 MHz. Linear frequency modulated (LFM) pulse widths and duty cycles in the table are reported without this modification. Bandwidths of pulsed continuous wave (CW), LFM, and phase modulated (PM) pulses correspond to reciprocal pulse width, "chirp width", and reciprocal sub-pulse width, respectively.

Table A-4. Interfering signals. Continuous refers to the interfering signal being present during the entire antenna scan. Gated refers to the interfering signal being present only when the targets are present. Pulsed signals are identified by the modulation type and pulse width/pulse repetition frequency. Ultra-wideband (UWB) signals are identified by their PRF. CW refers continuous wave, FM refers to frequency modulated, PM refers to phase modulated, BW refers to bandwidth, DC refers to duty cycle, QPSK refers to quadrature phase shift keying, QAM refers to quadrature amplitude modulation, OFDM refers to orthogonal frequency division modulation.

Interfering Signal	BW (MHz)	DC (%)	A[5]	F	B	D	C	E
QPSK	1	100	cont					
16 QAM	7	100			cont		cont	
64 QAM	7	100			cont		cont	
CDMA 2000	1	100			gated	gated	gated	gated
W-CDMA	5	100			gated	gated	gated	gated
OFDM	N/A	100		gated				
Pulsed UWB								

[5] Additional pulsed CW measurements are documented in [A-3] under radar B.

Interfering Signal	BW (MHz)	DC (%)	A[5]	F	B	D	C	E
100 kHz	>500	<0.1			gated			
1 MHz	>500	<0.1			gated			
10 MHz	>500	<0.1			gated			
Pulsed CW								
1us/1.0 kHz	1	0.1			gated	gated	gated	gated
2us/0.5 kHz	0.5	0.1			gated		gated	gated
1us/10.0 kHz	1	1.0			gated	gated	gated	gated
2us/5.0 kHz	0.5	1.0			gated		gated	gated
1 us/8-200 kHz	1	1.0-20.0		gated				
Pulsed LFM								
10 us/0.750 kHz	10	0.75		gated				
10 us /0.750 kHz	50	0.75		gated				
10 us/5.0 kHz	660	0.50		gated				
10 us /2.0 kHz	400	0.2		gated				
80 us /4.5 kHz	400	0.360		gated				
10 us /0.515 kHz	45	0.515		gated				
10 us /5.15kHz	460	5.15		gated				
Pulsed PM								
0.64 us/1.6 kHz	20.4	0.1		gated				
20 us/1.6 kHz	0.650	0.3		gated				

A.3 Procedure

Two different procedures, quantitative and qualitative, were used to evaluate the effects of interference. The quantitative procedure was used with radars B and D. This procedure estimated Pd by injecting 10 targets over 50 antenna rotations, i.e. 500 total targets, and counting the number visible to the operator. The procedure began by establishing a baseline signal to noise ratio and threshold with nominal Pd and Pfa, respectively. Then interfering signal power was incrementally increased while targets were counted and Pd was estimated. The IPC is the INR needed to drive the Pd outside the estimate's standard deviation.

The report noted that Pd estimation was possible with radars B/D because the effect of the interference on individual targets was observable. In other words the targets could be seen to disappear individually as interference power was increased. However, this radar did not have CFAR so most of the target disappearance happened near the center of the display where false alarms concentrate and obscure targets. Hence, it is more of an estimate of Pfa as opposed to Pd.

The qualitative procedure was used for radars A, F, and C/E. With these radars the continuous interfering signals caused the targets to dim equally no matter where they were along the target radial. This dimming increased with interference power to the point where all targets disappeared from the display. This effect trivialized quantitatively counting missed targets and the

corresponding degradation in Pd. In effect Pd went from 100% to 0% with nothing in between. The report did not say what caused this dimming phenomenon but it is presumed to be the result of display processing. In this case IPC were determined from a qualitative assessment of 20 or more radar display photographs at each of the interference levels.

A.4 Results

IPC results in terms of interference to noise ratio (INR) are listed in Table A-5. These results show IPC for continuous signals was significantly less than 0 dB meaning the interference power needs to be significantly less than noise power. Interference in radars B/D and C/E from pulsed signals with duty cycles as high as 1% was never observed with INR on the order of 40 dB. However, interference in radar F was observed at 20 dB INR when the duty cycle exceeded 5%. As expected, the results also show there is no difference between S and X band radars that share the same receiver signal processor and display.

The authors stated that differences in locations of preselector and LNA (A, F, and B/D are mounted below deck and C/E is mounted on top of the mast) and log amps and video detectors (B/D has them in separate boxes) may have some effect on IPC. However, no reason to expect this difference was provided.

Table A-5. IPC results in terms of INR.

Radar Designator	Procedure	Continuous IPC (dB)	Pulsed IPC (dB)
A	Qualitative	-7	NA
F	Qualitative	-6	20 for d.c. > 5 %
B/D	Quantitative	-12	NA>39
C/E	Qualitative	-9	NA>40

A.5 Discussion

While cochannel continuous interfering signals created significant interference at relatively low power levels the MSR was mostly unaffected by the co-channel pulsed interfering signals used. Off-tuning should provide even more compatibility.

The report states the measurement's ultimate goal was to determine 1) IPC for continuous and pulsed signals and 2) the effectiveness of MSR interference reduction techniques. While the first goal was met for the interfering signals used the second goal was not entirely met because measurements were not made without IR and scan to scan correlation.

Future work can improve upon this effort by

1) Expanding pulsed signals to include longer pulse widths and higher duty cycles corresponding to those used by todays solid state transmitter MSR

2) Replacing visual quantitative and qualitative visual performance measurement method with either built in test equipment (BITE) or simulation methods. Perhaps these methods can circumvent the target "dimming" problem encountered in this effort

3) Performing tests without IR and scan to scan correlation so performance with and without them can be quantified

A.6 References

[A-1] F. Sanders; R. Sole; B. L. Bedford; D. Franc; T. Pawlowitz, "Effects of RF Interference on Radar Receivers," NTIA Technical Report TR-06-444, Feb. 2006. Available https://www.its.bldrdoc.gov/publications/2481.aspx

[A-2] Report ITU-R M.2050, (2004), Test results illustrating the susceptibility of maritime radio navigation radars to emissions from digital communication and pulsed systems in the bands 2900-3100 and 9200-9500 MHz,International Telecommunications Union, Geneva, Switzerland.

[A-3] Report ITU-R M.2032, (2003), Tests illustrating the compatibility between maritime radio navigation radars and emissions from radiolocation radars in the band 2900-3100 MHz,International Telecommunications Union, Geneva, Switzerland.

APPENDIX B RADAR TO RADAR INTERFERENCE MITIGATION FACTORS

A number of factors mitigate radar to radar interference [B-1], [B-2]. These factors can be categorized by the radar component where they reside as shown in Table B-1.

Table B-1. Interference Mitigation Factors

Radar component	Factor	Note	Used in Report
Antenna			
	Antenna pattern coupling	Main and side lobes	Yes
Receiver			
	Selectivity	Detection filtering	Yes
	Spurious response suppression	Radio and intermediate frequency filtering	No
Signal Processor			
	Fast Time Constant (FTC) precipitation clutter rejection	Shortens interfering pulses	No
	Off tuning or frequency shifting	Shortens interfering pulses	Yes
	Linear or binary integration	Linear integrators such as the analog moving window are less effective against strong pulsed interference. Binary integrators such as the M/N threshold detector are more effective.	Binary integration
	Pulse removal or Interference Rejection (IR)	Removes interfering pulses with different pulse characteristics	PRI discrimination
	Hard limiting	Attenuates strong signals	No
	Log amplification	Similar effect as hard limiting	No
	Sensitivity Time Constant (STC) clutter rejection	Compensates for propagation loss. Attenuation of short range signals, clutter, and interference is significant.	No
	Constant False Alarm Rate (CFAR) threshold setting	Diminishes influence of pulsed interference on video threshold	Manual threshold
Display			
	Track while scan	Removes clutter by deleting targets with unlikely paths	No
	Scan to scan correlation	Removes clutter by deleting targets that disappear from scan to scan	No
	Dimming	Reduces weak signal brilliance	No

B.1 References

[B-1] Report ITU-R M.2076, (2006), Factors that mitigate interference from radiolocation Earth exploration-satellite service/ space research service (active) radars to maritime and aeronautical radio navigation radars in the 9.0-9.2 and 9.3-9.5 GHz bands and between Earth exploration-satellite service/ space research service (active) radars and radiolocation radars in the 9.3-9.5 and 9.8-10.0 GHz bands,International Telecommunications Union, Geneva,Switzerland

[B-2] Recommendation ITU-R M.1372-1, (2003), Efficient use of the radio spectrum by radar stations in the radio determination service,International Telecommunications Union, Geneva,Switzerland.

APPENDIX C UNCERTAINTY

C.1 Probability of error uncertainty

The simulation experiment can be modeled as a series of Bernoulli trials whose true probability of an error is p. The error probability estimator is

$$\hat{p} = \frac{n}{N} \tag{C-1}$$

where n is the number of errors in N independent trials.

As N goes to ∞ the estimator converges to the true value by the law of large numbers

$$\mathcal{E}(\hat{p}) = p \tag{C-2}$$

where $\mathcal{E}(\cdot)$ is the expectation operator. If the errors are independent, the variance of the estimator is

$$Var(\hat{p}) = {p(1-p)}/{N} \tag{C-3}$$

Furthermore, the probability that p lies within a confidence interval can be estimated

$$P[y_l \leq p \leq y_u] = 1 - \alpha \tag{C-4}$$

where y_l and y_u are the lower and upper confidence levels dependent on $\hat{p}$ and N, α is the error, and $1 - \alpha$ is the confidence. This probability is computed with a number of methods including the Clopper-Pearson, Wald, and Wilson score.

C.2 Fractional Coincidence

The fraction of coincidence is the probability that asynchronous pulses will overlap [C-1]. It is determined by

$$f_c = PRF_i(\tau_v + \tau_i) \tag{C-5}$$

under the condition that

$$\tau_i < PFI_v - \tau_v \tag{C-6}$$

and

$$\tau_v < PRI_i - \tau_i \tag{C-7}$$

where PRF is the pulse repetition frequency, PRI is the pulse repetition interval, τ is the pulse width, and the subscripts v and i are for victim and interfering, respectively.

Using linear superposition, this equation can be extended to a composite interfering waveform with multiple pulses, as is used in solid state maritime surveillance radars

$$f_c = PRF_i \sum_{k=1}^{n} (\tau_v + \tau_{ik}) \tag{C-8}$$

where PRF_i is the pulse repetition frequency of the composite waveform, τ_{ik} is the k-th interfering pulse width, and n is the total number of composite waveform pulses.

Fractional coincidence can be used to estimate the number of asynchronous pulsed interference events needed to obtain a specified uncertainty from the number required with continuous interference

$$N_{pulsed} = \frac{N_{continuous}}{f_c} \tag{C-9}$$

It has also been proposed, but not proved, that fractional coincidence can also be used to estimate pulsed interference INR from continuous interference INR [C-2]

$$INR_{pulsed} = INR_{continuous} - 10\log(f_c) \tag{C-10}$$

C.3 Asynchronous Period

The asynchronous period is computed to make sure we have enough independent interference events between the times when the asynchronous pulse trains periodically resynchronize. The period over which they resynchronize is determined by the least common multiple (LCM) of the two individual pulse periods.

As an example, assume one pulse train repeats every $m\Delta t$ seconds and the other every $n\Delta t$ seconds where Δt is a time increment and m and n are integers. The first pulse train will then repeat every $LCM(m,n)/m$ of its periods, the second pulse train will repeat every $LCM(m,n)/n$ of its periods, and the two will realign in $LCM(m,n)\Delta t$ seconds.

C.4 References

[C-1] Recommendation ITU-R RS.1280 (1997), *Selection of active space borne sensor emission characteristics to mitigate the potential for interference to terrestrial radars operating in frequency bands 1-10 GHz*, International Telecommunications Union,Geneva, Switzerland, Section 3 Interference criteria for terrestrial radars.

[C-2] Recommendation ITU-R M.1849 (2009), *Technical and operational aspects of ground based meteorological radars*, International Telecommunications Union,Geneva, Switzerland, Section 8.4.2 Impact of pulsed interference.

NTIA FORM 29
(4-80)

U.S. DEPARTMENT OF COMMERCE
NATIONAL TELECOMMUNICATIONS AND INFORMATION ADMINISTRATION

BIBLIOGRAPHIC DATA SHEET

1. PUBLICATION NO.	2. Government Accession No.	3. Recipient's Accession No.
TR-21-556		

4. TITLE AND SUBTITLE	5. Publication Date
Solid-state Marine Radar Interference in Magnetron Marine Radars	
	6. Performing Organization Code NTIA/ITS.T

7. AUTHOR(S)	9. Project/Task/Work Unit No.
R.J. Achatz, N. Kent, and E. Hill	
8. PERFORMING ORGANIZATION NAME AND ADDRESS Institute for Telecommunication Sciences National Telecommunications & Information Administration U.S. Department of Commerce 325 Broadway Boulder, CO 80305	08 6798 000 300
	10. Contract/Grant Number.

11. Sponsoring Organization Name and Address	12. Type of Report and Period Covered
U.S. Coast Guard Spectrum Management Telecommunications Policy Division U.S. Coast Guard CG-652 2100 2nd St. SW Stop 7101 Washington DC 20593-7101	

14. SUPPLEMENTARY NOTES

15. ABSTRACT (A 200-word or less factual summary of most significant information. If document includes a significant bibliography or literature survey, mention it here.)

Previously published field test results showed frequent solid state marine radar (SS-MR) interference in magnetron marine radars (M-MRs) at 0.34 nautical miles distance separation and 55 MHz frequency separation. The interference was mitigated but not completely eliminated by increasing distance separation, activating interference rejection (IR), and increasing frequency separation. This report describes a simulation and analysis method that can emulate the field test and uses the method to evaluate the previously published field test results. Results from the method support those of the field test to a large extent although the method results showed more complete mitigation with frequency separation and IR. The field test was performed with a single SS-MR interferer. Legacy M-MR IR may not be as effective in crowded ports or harbors where there are a number of new SS-MR operating nearby. In addition, new SS-MR signals may have higher duty cycles than the ones used here. This method will be an invaluable tool for determining the necessary frequency separation between legacy M-MR and new SS-MR.

16. Key Words (Alphabetical order, separated by semicolons)

interference, interference protection criteria, magnetron marine radar, marine radar, radio navigation radar, radio surveillance radar, solid state marine radar

17. AVAILABILITY STATEMENT	18. Security Class. (This report)	20. Number of pages
☒ UNLIMITED.	Unclassified	65
☐ FOR OFFICIAL DISTRIBUTION.	19. Security Class. (This page)	21. Price:
	Unclassified	N/A

NTIA FORMAL PUBLICATION SERIES

NTIA MONOGRAPH (MG)

A scholarly, professionally oriented publication dealing with state-of-the-art research or an authoritative treatment of a broad area. Expected to have long-lasting value.

NTIA SPECIAL PUBLICATION (SP)

Conference proceedings, bibliographies, selected speeches, course and instructional materials, directories, and major studies mandated by Congress.

NTIA REPORT (TR)

Important contributions to existing knowledge of less breadth than a monograph, such as results of completed projects and major activities.

JOINT NTIA/OTHER-AGENCY REPORT (JR)

This report receives both local NTIA and other agency review. Both agencies' logos and report series numbering appear on the cover.

NTIA SOFTWARE & DATA PRODUCTS (SD)

Software such as programs, test data, and sound/video files. This series can be used to transfer technology to U.S. industry.

NTIA HANDBOOK (HB)

Information pertaining to technical procedures, reference and data guides, and formal user's manuals that are expected to be pertinent for a long time.

NTIA TECHNICAL MEMORANDUM (TM)

Technical information typically of less breadth than an NTIA Report. The series includes data, preliminary project results, and information for a specific, limited audience.

For information about NTIA publications, contact the NTIA/ITS Technical Publications Office at 325 Broadway, Boulder, CO, 80305 Tel. (303) 497-3572 or e-mail ITSinfo@ntia.gov.